G M. SINCLAIR LIBRARY
UNIVERSITY OF HAWAII

Section B, Vol. 9

No. 3

APPLIED SCIENTIFIC RESEARCH

B. ELECTROPHYSICS, ACOUSTICS, OPTICS, MATHEMATICAL METHODS

Reports published under the auspices of

The Central National Organization for Applied Scientific Research in the Netherlands (T.N.O.)

The Netherlands Physical Society, Section for Applied Physics

The Royal Institute of Engineers of the Netherlands, Section for Technical Scientific Research

The Mathematical Centre, Amsterdam

R. Kronig, In Memoriam H. B. Dorgelo 169

L. B. Felsen, High-frequency diffraction by a wedge with a linearly varying surface impedance 170

Chester J. Marcinkowski, Some diffraction patterns of an absorbing half-plane 189

Letter to the editor *M. J. A. Bakker* and *J. Smidt*, A "Wonderstone" microwave cavity for electron spin resonance spectrometers 199

A. S. Gupta, Shear flow of a viscous infinitely electrically conducting fluid past a porous flat plate in the presence of a transverse magnetic field 201

M. v. Ments, Some phenomena occurring in floating battery systems . . . 205

W. I. Axford, Axisymmetric stagnation point flow in magnetohydrodynamics 213

L. M. Hocking, The flow of a conducting fluid past a magnetized cylinder at high magnetic Reynolds numbers 230

THE HAGUE
MARTINUS NIJHOFF
1961

APPLIED SCIENTIFIC RESEARCH has as its objective the publication of original investigations in the realm of the applied natural sciences. It is at present issued in two sections:

- *A*. containing papers on applied mechanics, hydro- and aeromechanics, heat and the mechanical and thermal properties of materials;
- *B*. containing papers on applied electrophysics, acoustics, optics and the electrical, acoustical and optical properties of materials.

In each section one volume will comprise 480 pages and will consist of six issues of 80 pages each, published at irregular intervals. It is estimated that the publication of one complete volume will require about $1\frac{1}{2}$ years. The subscription price is *f* 30 per volume for each section. Students may subscribe through the Secretary of the Governing and Editorial Board (address below) at the reduced price of 25 guilders.

Articles are accepted only if they deal with original research, not yet published elsewhere. They should preferably be written in English, but papers in French or German will also be accepted. Manuscripts must be typewritten, double spaced, on one side of the paper only. Illustrations should be in such form that plates can be made from them directly, the necessary ratio of reduction being if possible the same for all figures of the same article. The articles should be as concise as possible and should be preceded by a brief summary. The use of the rationalized practical system of units, which is based on the m, kg-mass and s, is recommended.

No honorarium is paid to contributors, but authors are entitled to 75 free reprints. Additional reprints may be obtained at a fixed price on prepublication order.

Governing Board:
Prof. ir J. J. Broeze, Delft.
Prof. dr R. Kronig, Delft.
Prof. dr H. W. Julius, The Hague.
Dr G. H. Reman, Amsterdam.
Prof. dr ir A. van Wijngaarden, Amsterdam.

Editorial Board:
Prof. dr L. J. F. Broer, Delft (General Editor).
Prof. dr ir C. B. Biezeno, Delft.
Dr W. de Groot, Eindhoven.
Prof. dr H. A. Lauwerier, Amsterdam.

National Editors:
Prof. dr G. Borelius, Stockholm, for Sweden.
Prof. dr A. van Itterbeek, Louvain, for Belgium.
Prof. J. Rybner, Copenhagen, for Denmark.
Prof. dr M. J. O. Strutt, Zürich, for Switzerland.
Prof. dr S. Westin, Trondheim, for Norway.

Articles should be sent to *the Secretary*, ir W. A. Welling, Laboratorium voor Aero- en Hydrodynamica, Rotterdamseweg 145, Delft, Netherlands.

Overnemen van de artikelen is verboden (Art. 15, al. 3, Auteurswet 1912)
Copyright 1961. All rights reserved

PRINTED IN THE NETHERLANDS

Digitized by the Internet Archive
in 2023 with funding from
Kahle/Austin Foundation

https://archive.org/details/applied-scientific-research_1961_9_3

H. B. DORGELO

IN MEMORIAM H. B. DORGELO

The death on 6th March 1961 of Professor Dr. H. B. Dorgelo, rector magnificus of the Technological University of Eindhoven, was a severe loss to the Dutch scientific world in general and to this journal in particular. Dorgelo was one of the founders of Applied Scientific Research directly after the second world war, and as chairman of the Governing Board he actually helped to overcome the numerous obstacles that lie in the way of a new publication. From the very beginning the emphasis was laid on the international character of the journal and it may be said without hesitation that by now this intention has been fully realized. As General Editor I had often occasion to consult Dorgelo on whose full support I could always count. Now that I am taking over his task in the Governing Board and turning over the Editorship I wish to express the hope that Applied Scientific Research may be a lasting memorial to a man who gave himself wholeheartedly to his task.

R. Kronig

Appl. sci. Res. Section B, Vol. 9

HIGH-FREQUENCY DIFFRACTION BY A WEDGE WITH A LINEARLY VARYING SURFACE IMPEDANCE

by L. B. FELSEN

Office of Naval Research, London Branch, London, England

Summary

A previously derived formal solution for the two-dimensional Green's function for a wedge with a linearly varying surface impedance is examined in the quasi-optic range of frequencies. An asymptotic representation, valid both in the illuminated and shadow regions, is derived for the scattered field due to an incident plane wave, and its properties are analyzed as a function of the rate of variation of surface impedance. A geometric-optical interpretation of the solution is emphasized.

§ 1. *Introduction.* As noted in a previous publication[1]), the two-dimensional problem of diffraction by a wedge with a linearly varying surface impedance (or admittance, depending on the polarization of the incident wave) can be solved by the conventional method of separation of variables, and the solution can be presented in alternative forms which are advantageous for different investigations. A radial transmission formulation has been found useful for the analysis of radiation from a tapered surface wave antenna[2]), the surface impedance of which varies in the above-described manner. In this paper, an angular transmission formulation is utilized to determine the scattering properties of the variable impedance wedge in the quasi-optic wavelength range. The diffracted field due to an incident plane wave, observed far from the edge, is expressed in the shadow region in terms of an asymptotic expansion involving terms of the form $(k\rho)^{-m-\frac{1}{2}} I_m(\phi, \phi')$, $m = 0, 1, 2, \ldots$, where k is the free-space wavenumber, (ρ, ϕ) the cylindrical coordinate of the observation point and ϕ' the incident wave direction. The angular function $I_m(\phi, \phi')$, which also depends on the rate of impedance variation on the wedge, is given in terms of an integral and, for $m \geqslant 1$, is derivable via a recursive procedure from a knowledge of $I_0(\phi, \phi')$. Explicit expressions for I_0 are obtained for two special cases: 1) a wedge having a linearly varying surface impedance on one side and a "perfect absorber" of the Sommerfeld type on the other side, and 2) a wedge having a purely reactive impedance with the same rate of (linear) variation on both sides, but with the algebraic sign of the reactance on one side being the opposite of that on the other. In the illuminated region, the asymptotic evaluation, carried out to $O(1/\sqrt{k\rho})$, yields a reflected geometric-optical field in addition to the diffracted contribution.

While the variable impedance wedge configuration described herein might conceivably serve as a model for the analysis of diffraction by sharp mountain ridges with certain variable properties, or by high-speed vehicles in the upper atmosphere surrounded by a plasma sheath with a certain variable density, the main purpose of this investigation has been the comparison of the rigourous asymptotic solution in the quasi-optic range with predictions based on generalized geometric-optical procedures. Such procedures have been employed with considerable success by Keller and his co-workers [3]) for the analysis of diffraction by relatively arbitrary structures. In Keller's geometrical theory of diffraction, the scattered field as $k \to \infty$ is viewed as arising from various types of reflected and diffracted rays, whose amplitudes are determined by the properties of the obstacle surface "at" the point of emergence of a given ray. If this model is to be applied to the analysis of diffraction problems at large but finite values of k, it is evident that the word "at" employed above should be replaced by "in the neighbourhood of", with the expectation that a slow variation of surface properties in an interval of a wavelength does not invalidate the local analysis of the quasi-optic scattering process. Since there is no precise estimate of what constitutes a slow variation, it is pertinent to investigate specific structures exhibiting different types of variability of surface properties and to examine the dependence of these solutions on the rate of variation. The present problem is suited to an analysis of the effect of a variable surface impedance in the vicinity of an edge singularity.

If the surface admittance varies like $A\rho$, where A is a constant (which may have different values on the two wedge faces) and ρ is the distance from the apex, it is found that the diffracted wave amplitude for $A \ll 1$ is essentially the same as that for a zero admittance wedge (although the wedge admittance tends to infinity as $\rho \to \infty$), while the diffracted wave amplitude for $A \gg 1$ is essentially that for an infinite admittance wedge. $A \ll 1$ and $A \gg 1$ correspond, respectively, to slow and rapid admittance variations near $\rho = 0$. One notes that in the former case the diffracted wave amplitude is determined properly by the zero admittance value "at" the point of diffraction $\rho = 0$, while in the latter case the edge admittance is of no consequence. For the two special cases mentioned at the end of the first paragraph, a study of the diffracted wave amplitude as a function of A can be carried out explicitly to determine over what range the quasi-optic approximation (involving the point of diffraction only) yields results acceptable to within some definite criterion of accuracy.

The utility of an angular transmission analysis of certain wedge problems, involving the use of the Kontorovitch-Lebedev transform, has been emphasized previously 4) 5). In the present context, the angular domain is not restricted to the region $0 \leqslant \phi \leqslant \alpha$ bounded by the two half planes forming the wedge, but is allowed to range from $\phi = -\infty$ to $\phi = \infty$. The requisite boundary conditions at $\phi = 0, \alpha$ are then restored by superposing in the infinite angular domain an infinite set of "image" solutions. While the infinite angular space concept has been exploited primarily for the analysis of diffraction by curved objects 6) 7), its considerable utility in connection with structures possessing edge or tip singularities 1) is not to be overlooked. In fact, a prime virtue of this type of analysis (not sufficiently emphasized in the literature) is a resulting formulation which permits the immediate identification of geometrically reflected, and of diffracted, field contributions in an asymptotic evaluation at high frequencies.

§ 2. *Formal solution.* It was shown in 1) that the electromagnetic fields radiated by a line source of electric or magnetic currents in the presence of the variable impedance wedge (see fig. 1) can be inferred from a scalar Green's function G. The impedances

$\hat{z}_{0,\alpha}$ at the wedge faces $\phi = 0, \alpha$ have the form

$$\hat{z}_{0,\alpha} = \begin{cases} Z_0\, ik\rho c_{0,\alpha} \text{ for a line source of electric currents,} \\ Z_0/ik\rho c_{0,\alpha} \text{ for a line source of magnetic currents,} \end{cases}$$

where $Z_0 = \sqrt{\mu/\varepsilon}$ is the characteristic impedance of free space, ρ the radial variable, k the free-space wavenumber, and c_0, c_α are constants restricted such that $\operatorname{Im} c_{0,\alpha} \leqslant 0$. (A time dependence $\exp(-i\omega t)$ is assumed throughout). G satisfies the boundary condition $G = \mp c_{0,\alpha}(\partial G/\partial\phi)$ at $\phi = 0, \alpha$.

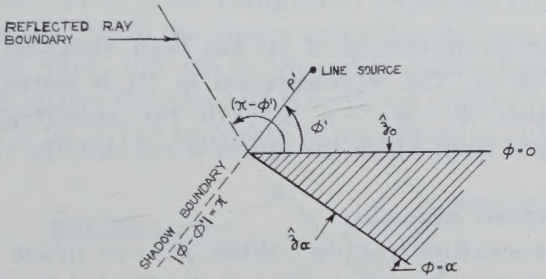

Fig. 1. Physical configuration and various geometric-optical domains.

For a study of the high-frequency diffraction properties of the wedge surface, the Green's function G is most conveniently expressed in terms of the angular transmission (radial eigenfunction) representation in (22) of 1):

$$G(\underline{\rho}, \underline{\rho}') =$$

$$= \tfrac{1}{4} \int_0^{i\infty} \mu(1-e^{i2\mu\pi}) H_\mu^{(1)}(k\rho) H_\mu^{(1)}(k\rho') G_\phi(\phi, \phi'; \mu^2)\, d\mu,\ |\phi - \phi'| > \pi. \quad (1)$$

The angular characteristic Green's function G_ϕ is given in closed form by (12) of 1):

$$G_\phi(\phi, \phi'; \mu^2) = \frac{(e^{-i\mu\phi_<} + \Gamma_0\, e^{i\mu\phi_<})(e^{-i\mu(\alpha-\phi_>)} + \Gamma_\alpha\, e^{i\mu(\alpha-\phi_>)})}{-\,2i\mu(e^{-i\mu\alpha} - \Gamma_0\Gamma_\alpha\, e^{i\mu\alpha})} \qquad (2)$$

$$\Gamma_0 \equiv \Gamma_0(\mu) = \frac{i\mu c_0 - 1}{i\mu c_0 + 1}, \quad \Gamma_\alpha \equiv \Gamma_\alpha(\mu) = \frac{i\mu c_\alpha - 1}{i\mu c_\alpha + 1}, \qquad (3)$$

where $\phi_<$ and $\phi_>$ denote the lesser and greater, respectively, of the variables ϕ and ϕ'. Alternatively, G_ϕ can be expressed in terms of images in an infinitely extended angular transmission line as in (13) of [1]):

$$G_\phi(\phi, \phi'; \mu^2) = G_{\phi\infty}(\phi, \phi') + \sum_{n=1}^{\infty} \Gamma_0^{n-1}\Gamma_\alpha^n G_{\phi\infty}(\phi, 2n\alpha - \phi') + \\ + \sum_{n=1}^{\infty} (\Gamma_\alpha\Gamma_0)^n [G_{\phi\infty}(\phi, 2n\alpha + \phi') + G_{\phi\infty}(\phi, -2n\alpha + \phi')] + \\ + \sum_{n=0}^{\infty} \Gamma_\alpha^n \Gamma_0^{n+1} G_{\phi\infty}(\phi, -2n\alpha - \phi'), \ \operatorname{Im}\mu > 0, \tag{4}$$

where

$$G_{\phi\infty}(\phi, \phi') = \frac{e^{i\mu|\phi-\phi'|}}{-2i\mu}, \quad \operatorname{Im}\mu > 0. \tag{5}$$

The physical interpretation of (4) has been discussed previously (see fig. 4 of [1])). The representation in (1) is restricted to the angular region $|\phi - \phi'| > \pi$, i.e., to the geometrical shadow region of fig. 1 from which the source is not directly visible.

§ 3. *Asymptotic evaluation.*

1. In the shadow region. When $\rho' \to \infty$ (plane wave incidence) and $k\rho \gg 1$, we may represent the Hankel functions in (1) by their large argument asymptotic formulae

$$H_\mu^{(1)}(k\rho') \sim \sqrt{\frac{2}{\pi k\rho'}}\, e^{i(k\rho' - \frac{1}{2}\mu\pi - \frac{1}{4}\pi)}, \ \rho' \to \infty, \tag{6}$$

$$H_\mu^{(1)}(k\rho) \sim \sqrt{\frac{2}{\pi k\rho}}\, e^{i(k\rho - \frac{1}{2}\mu\pi - \frac{1}{4}\pi)} \sum_{m=0}^{\infty} \frac{(\mu, m)}{(-2ik\rho)^m}, \quad k\rho \gg |\mu|, \tag{7}$$

$$(\mu, m) \equiv \frac{[4\mu^2 - 1^2][4\mu^2 - 3^2]\ldots[4\mu^2 - (2m-1)^2]}{2^{2m} m!}, \ (\mu, 0) \equiv 1. \tag{8}$$

Since the integrand in (1) is exponentially damped for large values of μ when $|\phi - \phi'| > \pi$ (see (9) of [1]) and (4)), the error incurred by employing (7) over the entire range in μ can be shown to be exponentially small and therefore negligible. The field in the shadow region is therefore given asymptotically by

$$G(\underline{\rho}, \underline{\rho}') \sim A(k\rho')A(k\rho) \sum_{m=0}^{\infty} \frac{I_m(\phi, \phi')}{(-2ik\rho)^m}, \ \rho' \to \infty, \ k\rho \gg 1, \tag{9}$$

where

$$A(x) = \sqrt{\frac{2}{\pi x}}\, e^{i(x - \frac{1}{4}\pi)}, \tag{10}$$

$$I_m(\phi, \phi') = -\tfrac{1}{2} i \int_0^{i\infty} \mu(\mu, m) \sin \mu\pi G_\phi(\phi, \phi'; \mu^2)\, d\mu. \tag{11}$$

Since

$$(\mu, m) = \frac{1}{m}\left[\mu^2 - \tfrac{1}{4} - m(m-1)\right] (\mu, m-1), \tag{12}$$

and $(d^2/d\phi^2)G_\phi = -\mu^2 G_\phi$, $\phi \neq \phi'$, it follows that the I_m can also be obtained from I_0 through use of the recursion formula [8])

$$I_m = -\frac{1}{m}\left[\frac{\partial^2}{\partial\phi^2} + m(m-1) + \tfrac{1}{4}\right] I_{m-1}, \quad m = 1, 2 \ldots \tag{13}$$

From the nature of the factors $A(k\rho')A(k\rho)$ in (9) it is noted that the diffracted field in the shadow region has the form of an outgoing cylindrical wave, and can be viewed as arising from the incident ray which strikes the edge and is scattered radially in all directions as shown in fig. 2. The amplitude of the diffracted rays as a function of ϕ, ϕ' and the surface properties is given by $I_m(\phi, \phi')$. Of particular interest is the dependence on the surface impedance $\hat{z}_{0,\alpha}$. Although the diffracted rays appear to emanate from the edge, their amplitude is determined by the impedance in a neighbourhood surrounding the edge. This becomes evident from an examination of I_m for the two extreme cases $c_{0,\alpha} \gg 1$ and $c_{0,\alpha} \ll 1$. For the case of a magnetic line source, for example, $\hat{z}_{0,\alpha} \to \infty$ as $\rho \to 0$ and $\hat{z}_{0,\alpha} \to 0$ as $\rho \to \infty$, for any finite value of $c_{0,\alpha}$. When $c_{0,\alpha} \ll 1$, the impedance decreases very slowly away from the edge; in the evaluation of I_m, one may set $\Gamma_{0,\alpha} \approx -1$ since the major contribution from the exponentially decreasing integrand arises from the range of small μ. The resulting diffracted wave amplitude is approximately that appropriate to an infinite impedance wedge. However, when $c_{0,\alpha} \gg 1$, the impedance decreases very rapidly away from the edge and the resulting I_m is approximately that corresponding to $\Gamma_{0,\alpha} \approx 1$, i.e., a zero

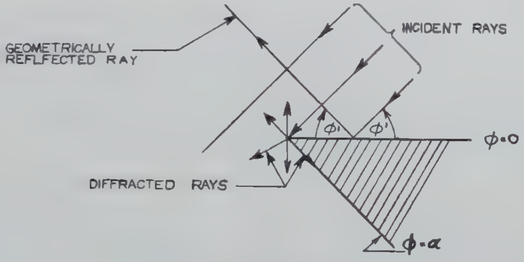

Fig. 2. Quasi-optic field contributions.

impedance wedge. Thus, it is noted that for slow impedance variation (per wavelength) near the edge the diffracted wave amplitude is essentially determined by the impedance "at" the edge, while for a rapidly varying impedance the properties at the edge are of no consequence and the diffracted wave amplitude is determined by the properties of the surface away from the edge.

To obtain a more precise estimate of what constitutes a slow or rapid impedance variation as employed above, we consider an auxiliary problem for which $\Gamma_\alpha = 0$. This implies that the surface at $\phi = \alpha$, instead of having a surface impedance $\mathfrak{z}_\alpha$, is a "perfect absorber for angularly propagating waves" (see remarks preceding (21) of [1])). G_ϕ as represented in (4) now comprises only the contributions from the source at $\phi = \phi'$ and an image source at $\phi = -\phi'$. Upon writing

$$\Gamma_0 = 1 - \frac{2}{i\mu c_0 + 1}, \tag{14}$$

one can evaluate I_0 in (11) as follows:

$$I_0(\phi, \phi') =$$

$$= \frac{1}{8}\left[\frac{1}{\pi + |\phi - \phi'|} + \frac{1}{\pi - |\phi - \phi'|} + \frac{1}{\pi + (\phi + \phi')} + \frac{1}{\pi - (\phi + \phi')}\right] -$$

$$- \frac{1}{4c_0}\Big[B(\phi + \phi' - \pi, c_0) - B(\phi + \phi' + \pi, c_0)\Big], \quad \Gamma_\alpha = 0, \tag{15}$$

where

$$B(x, c_0) = \int_0^\infty \frac{e^{-\nu x}}{\nu - \dfrac{1}{c_0}}\, d\nu = \tag{15a}$$

$$= e^{-x/c_0}\, E_1\!\left(-\frac{x}{c_0}\right), \quad E_1(y) = \int_y^\infty \frac{e^{-\nu}}{\nu}\, d\nu. \tag{15b}$$

The exponential integral $E_1(y)$ is a regular function of y in the complex y-plane cut along the negative real y axis. (15*b*) can likewise be considered as the analytic continuation of (15*a*) for complex and negative real values of x. $E_1(y)$ possesses the series representation [9])

$$E_1(y) = -\gamma - \ln y - \sum_{n=1}^{\infty} \frac{(-y)^n}{n!n}, \quad \gamma = 0.5772. \tag{16a}$$

For large y, successive integration by parts in (15b) yields the asymptotic formula

$$E_1(y) \sim \frac{e^{-y}}{y} \sum_{m=0}^{\infty} \frac{m!}{(-y)^m}, \quad |y| \to \infty, \ |\arg y| < \frac{3\pi}{2}. \tag{16b}$$

The exponential integral can also be expressed in terms of the sine and cosine integrals

$$\mathrm{Si}\,(y) = \int_0^y \frac{\sin t}{t}\,\mathrm{d}t, \quad \mathrm{Ci}\,(y) = \int_\infty^y \frac{\cos t}{t}\,\mathrm{d}t, \tag{16c}$$

as

$$E_1(-iy) = -\mathrm{Ci}\,(y) - i\,\mathrm{Si}\,(y) + \tfrac{1}{2}i\pi. \tag{16d}$$

For large values of c_0, use of (16a) yields

$$-\frac{1}{4c_0}[B(x_1, c_0) - B(x_2, c_0)] = -\frac{1}{4c_0}\left[\ln\frac{x_2}{x_1} + 0\left(\frac{1}{c_0}\right)\right], c_0 \gg 1, \tag{17a}$$

while for small values of c_0 (16b) leads to

$$-\frac{1}{4c_0}[B(x_1, c_0) - B(x_2, c_0)] = \frac{1}{4}\left(\frac{1}{x_1} - \frac{1}{x_2}\right) + 0(c_0), \ c_0 \ll 1. \tag{17b}$$

A plot of $Q(\beta) = \beta\, e^{-\beta} E_1(-\beta)$ for positive real, negative real, and negative imaginary values of β is shown in fig. 3, where $\beta = (x/c_0)$. Since x stands for $(\phi + \phi' \pm \pi)$ and is always real, the range of real values of β allows for positive and negative real values of c_0, i.e., purely reactive surface impedances. The negative imaginary values of β, on the other hand, account for positive real surface impedances when $x > 0$. It is noted for all cases that $|Q| < 0.05$ for $|\beta| < 0.01$ and $(1 - |Q|) < 0.05$ for $|\beta| > 20$. To facilitate an interpretation, let us rewrite (15) as

$$I_0(\phi, \phi') = \frac{1}{8}\left(\frac{1}{\pi + |\phi - \phi'|} + \frac{1}{\pi - |\phi - \phi'|}\right) - \\ - \frac{1}{8x_1}[1 + 2Q(\beta_1)] + \frac{1}{8x_2}[1 + 2Q(\beta_2)], \tag{18a}$$

$$Q(\beta) = \beta\, e^{-\beta} E_1(-\beta), \ \beta_{1,2} = \frac{x_{1,2}}{c_0}, \ x_{1,2} = \phi + \phi' \mp \pi. \tag{18b}$$

It is difficult to predict without detailed calculation via (18*a*) the effect of various values of c_0 on the magnitude of I_0 since the pertinent parameter is β which contains both ϕ, ϕ' and c_0. However, we can make the following statements regarding maximum effects: a) If $|\beta_{1,2}| < .01$, the coefficients of $(8x_{1,2})^{-1}$ differ in magnitude by at most 10 percent from unity. A coefficient equal to unity represents a value $c_0 = \infty$, i.e., a surface with infinite and zero impedance, respectively, for the electric and magnetic line source excitations. b) If $|\beta_{1,2}| > 20$, $2Q(\beta_{1,2})$ differs in magnitude from the value (-2) by at most 10 percent. A value of (-1) for the coefficients of $(8x_{1,2})^{-1}$ represents a value $c_0 = 0$, corresponding to a surface with zero and infinite impedance, respectively, for the electric and magnetic line source excitations.

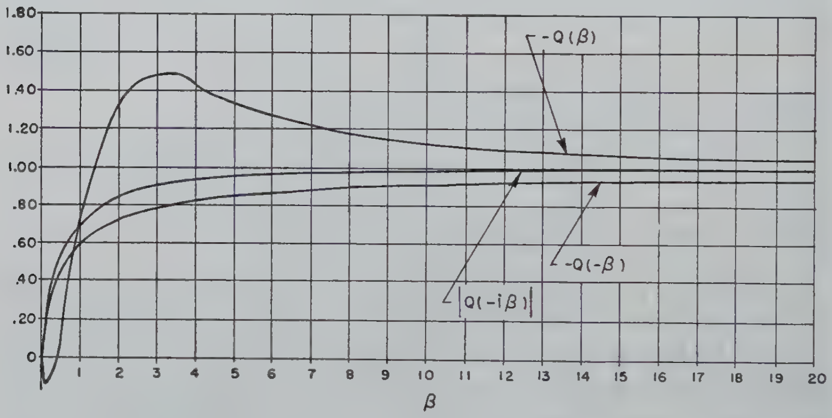

Fig. 3. Plot of $Q(\beta) = \beta\, e^{-\beta} E_1(-\beta)$.

2. In the illuminated region. To carry out an asymptotic field evaluation in the illuminated region $|\phi - \phi'| < \pi$, it is convenient to separate from the image representation (4) those terms for which $|\phi - \varphi| < \pi$, where φ is the location of a given source in the infinitely extended angular region. These terms alone can give rise to a geometric-optical field contribution, as shown below. If the wedge angle $\alpha > \pi$, the only sources in this category are those situated at $\varphi = \pm\phi'$, $2\alpha - \phi'$, where $0 \leqslant (\phi, \phi') \leqslant \alpha$. Thus, we write

$$G_\phi = \bar{G}_\phi + (G_\phi - \bar{G}_\phi), \tag{19a}$$

where

$$\bar{G}_\phi = G_{\phi\infty}(\phi, \phi') + \Gamma_0 G_{\phi\infty}(\phi, -\phi') + \Gamma_\alpha G_{\phi\infty}(\phi, 2\alpha - \phi'). \tag{19b}$$

Since $(G_\phi - \bar{G}_\phi)$ behaves for all $0 \leqslant (\phi, \phi') \leqslant \alpha$ like $\exp[-(Im\mu)\beta]$, $\beta > \pi$, when $\mu \to i\infty$, an asymptotic evaluation of the contribution from this term to the integral (1) is carried out as in (9) and yields only a diffracted wave effect. For an evaluation of the contribution from $\bar{G}_\phi$ in (19*b*), we examine separately each of the terms.

Contribution from $G_{\phi\infty}(\phi, \phi')$. Upon substituting $G_{\phi\infty}$ into (1), replacing $H_\mu{}^{(1)}(k\rho')$ by its asymptotic form (6), $H_\mu{}^{(1)}(k\rho)$ by its Sommerfeld integral representation [10])

$$H_\mu{}^{(1)}(k\rho) = \frac{1}{\pi}\int_{-\delta+i\infty}^{\delta-i\infty} \mathrm{d}\psi\, \mathrm{e}^{ik\rho\cos\psi}\, \mathrm{e}^{i\mu(\psi-\frac{1}{2}\pi)}, \quad \delta = 0^+, \tag{20}$$

performing an interchange of the orders of integration (permissible if $|\phi - \phi'| > \pi + \delta$) and carrying out the integration over μ, one obtains for the integral L_1 defined as follows:

$$L_1(|\phi - \phi'|) \equiv \tfrac{1}{4}\int_0^{i\infty} G_{\phi\infty}(\phi, \phi')\mu(1 - \mathrm{e}^{i2\mu\pi})\, H_\mu{}^{(1)}(k\rho)H_\mu{}^{(1)}(k\rho')\,\mathrm{d}\mu =$$

$$= A(k\rho')\,\frac{1}{8\pi}\int_{-\delta+i\infty}^{\delta-i\infty} \mathrm{d}\psi\, \mathrm{e}^{ik\rho\cos\psi} D(\psi, |\phi-\phi'|),\ \rho' \to \infty,\ |\phi - \phi'| > \pi + \delta. \tag{21}$$

$$D(\psi, |\phi - \phi'|) = \frac{1}{\pi - |\phi - \phi'| - \psi} + \frac{1}{\pi + |\phi - \phi'| + \psi}\,. \tag{21a}$$

Unlike the left-hand side of (21), the integral on the right-hand side is defined as well when the restriction $|\phi - \phi'| > \pi + \delta$ is removed. If the path of integration in the complex ψ-plane is chosen symmetrically with respect to the origin, the value of L_1 for $|\phi - \phi'| < \pi$ differs from that for $|\phi - \phi'| > \pi$ by the residue at the pole $\psi_p = \pi - |\phi - \phi'|$ as shown in fig. 4. Thus, for any $|\phi - \phi'|$

$$L_1(|\phi - \phi'|) = \frac{i}{4}\,A(k\rho')\Big[\mathrm{e}^{-ik\rho\cos(\phi-\phi')}\, H(\pi - |\phi - \phi'|) -$$

$$- \frac{i}{2\pi}\int_{-\delta+i\infty}^{\delta-i\infty} \mathrm{d}\psi\, \mathrm{e}^{ik\rho\cos\psi}\, D(\psi, |\phi - \phi'|)\Big], \tag{22}$$

where

$$H(x) = 1,\ x > 0;\ H(x) = 0,\ x < 0. \tag{22a}$$

It is noted from (22) that $G_{\phi\infty}$ contributes the incident field in the illuminated region $|\phi - \phi'| < \pi$, and that the diffracted field as represented by the integral has the same functional form (as a function of $|\phi - \phi'|$) for any $|\phi - \phi'|$. (For an incident plane wave of unit amplitude, the normalization $\frac{1}{4}iA(k\rho') = 1$ is employed).

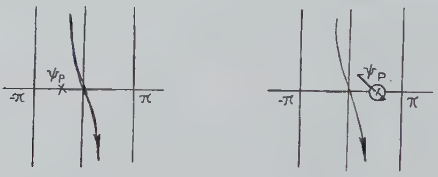

(a) $|\phi-\phi'|>\pi$ (b) $|\phi-\phi'|<\pi$

Fig. 4. Paths of integration in complex ψ-plane.

A steepest descent evaluation (through the saddle point at $\psi = 0$) of the integral in (22) for large values of $k\rho$ yields to $0(1/\sqrt{k\rho})$ and for all values of $|\phi - \phi'|$ [11])

$$L_1(|\phi - \phi'|) \sim \frac{i}{4} A(k\rho') \Big[\mathrm{e}^{-ik\rho\cos(\phi-\phi')}\, H(\pi - |\phi - \phi'|) -$$

$$- \frac{i}{2} A(k\rho) \left(\frac{1}{\pi - |\phi - \phi'|} + \frac{1}{\pi + |\phi - \phi'|} \right) - T(\rho, |\phi - \phi'|) \Big], \tag{23}$$

where

$$T(\rho,\varphi) = \frac{\mathrm{e}^{ik\rho}}{2} \operatorname{sgn}(\pi - \varphi) \left[F(\xi) - \frac{\mathrm{e}^{\frac{1}{4}i\pi}}{\xi\sqrt{2\pi}} \right],\quad \xi = \sqrt{k\rho}\left|\sin\frac{\pi - \varphi}{2}\right|, \tag{23a}$$

$$\operatorname{sgn}(\pi - \varphi) = \pm 1, \quad \varphi \lessgtr \pi. \tag{23b}$$

$F(\xi)$ is the function [12])

$$F(\xi) = \frac{2}{\sqrt{\pi}}\, \mathrm{e}^{-i2\xi^2} \int_{(1-i)\xi}^{\infty} \mathrm{d}x\, \mathrm{e}^{-x^2}, \tag{23c}$$

which behaves for large ξ like

$$F(\xi) \sim \frac{\mathrm{e}^{\frac{1}{4}i\pi}}{\xi\sqrt{2\pi}}, \quad \xi \gg 1. \tag{23d}$$

The first term inside the square brackets in (23) represents the incident field, the second term a diffracted contribution and the third term the transition effect near the shadow boundary $|\phi - \phi'| = \pi$. The extent of the transition region is defined approximately by $\xi \leqslant 4$; for $\xi > 4$, the asymptotic formula (23*d*) applies with good accuracy so that T in (23*a*) vanishes in that range. Since the transition region at $|\phi - \phi'| \approx \pi$ arises entirely from the contribution due to $G_{\phi\infty}(\phi, \phi')$ and does not contain a dependence on the impedance properties of the wedge, one notes that the light-shadow transition behaviour is independent of the wedge impedance.

Contribution from $\Gamma_0 G_{\phi\infty}(\phi, -\phi')$. Upon employing (14) and following the same procedure as above one obtains for the integral L_2 defined in the range $(\phi + \phi') > \pi$ as

$$L_2(\phi+\phi') \equiv \tfrac{1}{4}\int_0^{i\infty} \Gamma_0 G_{\phi\infty}(\phi, -\phi')\mu(1-\mathrm{e}^{i2\mu\pi})H_\mu{}^{(1)}(k\rho)H_\mu{}^{(1)}(k\rho')\,\mathrm{d}\mu \qquad (24)$$

the result $(\rho' \to \infty)$

$$L_2(\phi + \phi') = L_1(\phi + \phi') + L_2'(\phi + \phi');\ (\phi + \phi') > \pi, \qquad (25a)$$

$$L_2'(\phi + \phi') = -A(k\rho')\frac{1}{4\pi c_0}\int_{-\delta-i\infty}^{\delta-i\infty} \mathrm{d}\psi\, \mathrm{e}^{ik\rho\cos\psi}\, \cdot$$

$$\cdot\, [B(\phi + \phi' + \psi - \pi, c_0) - B(\phi + \phi' + \psi + \pi, c_0)], \qquad (25b)$$

where $L_1(\phi + \phi')$ and $B(x, c_0)$ are defined in (21) and (15*a*), respectively. The integrand in (25*b*) possesses branch points at $\psi_b = \pm\pi - (\phi + \phi')$ in view of (15*b*) and (16*a*). When $(\phi + \phi') > \pi$ both branch points occur to the left of the symmetrically chosen path of integration in the complex ψ-plane, and L_2' is defined

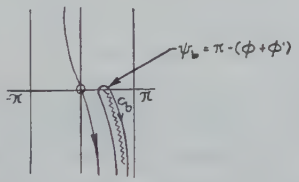

Fig. 5. Contours for I_2' when $(\phi + \phi') < \pi$.

as in (25*b*). When $(\phi + \phi') < \pi$, the value of L_2' differs from that in (25*b*) by the branch point, and associated branch cut, contribution due to $\psi_b = \pi - (\phi + \phi')$ as shown in fig. 5. The branch cut has been drawn so as to assure convergence of the integral along c_b as determined by the behavior of $\exp(ik\rho \cos\psi)$. Thus, for any value of $(\phi + \phi')$,

$$L_2(\phi + \phi') =$$
$$= L_1(\phi+\phi') + L_2'(\phi+\phi') + L_2''(\phi+\phi') H(\pi - (\phi+\phi')), \quad \rho' \to \infty, \tag{26a}$$

$$L_2''(\phi + \phi') =$$
$$= -A(k\rho') \frac{1}{4\pi c_0} \int_{c_b} \mathrm{d}\psi \, \mathrm{e}^{ik\rho\cos\psi} B(\psi - \psi_b, c_0), \quad \psi_b = \pi - (\phi + \phi'), \tag{26b}$$

where L_1 and L_2' are given in (22) and (25b), respectively.

To effect a simplification of L_2'' we introduce the change of variable

$$\psi = \psi_b - iz \tag{27}$$

so that

$$L_2''(\phi + \phi') = -\frac{iA(k\rho')}{4\pi c_0} \int_{c_b'} \mathrm{d}z \, \mathrm{e}^{ik\rho\cos(\psi_b - iz)} B(-iz, c_0), \tag{28}$$

where c_b' is a contour enclosing the branch cut along the positive real z axis in the positive sense. Upon substituting for $B(-iz, c_0)$ the exponential integral from (15b) and then the series expansion (16a), one notes that the only contribution to c_b' arises from the ($\ln z$) term since all the other terms in the series are continuous across the positive real z axis. Thus,

$$L_2''(\phi + \phi') = \frac{iA(k\rho')}{4\pi c_0} \int_{c_b'} \mathrm{d}z \, \mathrm{e}^{ik\rho\cos(\psi_b - iz)} \, \mathrm{e}^{iz/c_0} \ln z. \tag{29}$$

Finally, since

$$\ln (x\,\mathrm{e}^{i2\pi}) = \ln x + i2\pi, \tag{30}$$

one obtains for (29)

$$L_2''(\phi + \phi') = -\frac{A(k\rho')}{2c_0} \int_0^\infty \mathrm{d}x \exp[ik\rho\cos(\psi_b - ix) + ix/c_0] = \tag{31a}$$

$$= -\frac{A(k\rho')}{2c_0} \int_0^\infty \mathrm{d}x \exp\left[i\left(k\rho\cos\psi_b\cosh x + \frac{x}{|c_0|}\cos\gamma\right) - \right.$$
$$\left. - \left(k\rho\sin\psi_b\sinh x + \frac{x}{|c_0|}\sin\gamma\right)\right], \tag{31b}$$

where

$$c_0 = |c_0| \, e^{-i\gamma}, \quad 0 \leqslant \gamma \leqslant \pi. \tag{31c}$$

Since $\sin \psi_b > 0$ in the domain of existence of L_2'', the integrand is exponentially damped with increasing x.

An asymptotic evaluation of L_2 in (26*a*) for large values of $k\rho$ can now be carried out directly. The result for $L_1(\phi + \phi')$ is given in (23), and a saddle point evaluation of L_2' in (25*b*) to $0(1/\sqrt{k\rho})$ yields (B is a slowly varying function compared with $\exp(ik\rho \cos \psi)$)

$$L_2'(\phi+\phi') \sim$$
$$-\frac{1}{4c_0} A(k\rho')A(k\rho) \, [B(\phi+\phi' - \pi, c_0) - B(\phi + \phi' + \pi, c_0)]. \tag{32}$$

For an asymptotic evaluation of L_2'' one notes that the maximum contribution occurs in the neighborhood of $x = 0$. Upon expanding the exponent to $0(x)$ and carrying out the integration one obtains (note: $\psi_b = \pi - (\phi + \phi')$)

$$L_2''(\phi + \phi') \sim - \tfrac{1}{2} A(k\rho') \, e^{-ik\rho \cos(\phi+\phi')} \frac{1}{k\rho c_0 \sin(\phi + \phi') - i}. \tag{33}$$

Thus,

$$L_2(\phi+\phi') \sim \frac{i}{4} A(k\rho') \Big\{ \Gamma_0[k\rho \sin(\phi+\phi')] \, e^{-ik\rho \cos(\phi+\phi')} H(\pi - \phi - \phi') -$$
$$- \frac{i}{2} A(k\rho) \Big[\frac{1}{\pi - (\phi + \phi')} + \frac{1}{\pi + (\phi + \phi')} - \frac{2}{c_0} \cdot$$
$$\cdot \, (B(\phi + \phi' - \pi, c_0) - B(\phi + \phi' + \pi, c_0)) \Big] - T(\rho, \phi + \phi') \Big\}, \tag{34}$$

where $\Gamma_0(\mu)$ is defined in (3).

It is noted that for $|\phi - \phi'| > \pi$, (34) together with (23) agrees, as it must, with (15) and (9). Thus, the functional form of the diffracted wave contribution is the same for all geometric-optical domains. The expression for L_2 in (34) becomes infinite as $(\phi + \phi) \to \pi$, since the asymptotic evaluation of L_2' in (32) does not apply when the branch point approaches the saddle point at $\psi = 0$. However, the divergent term increases only logarithmically so that the affected wave amplitude behaves like

$$(1/\sqrt{k\rho}) \ln (\pi - \phi - \phi').$$

Since $k\rho \gg 1$, the excluded range of $(\pi - \phi - \phi')$, in which

$|\ln(\pi - \phi - \phi')|$ is $O(\sqrt{k\rho})$, is therefore very small. As in (9) and (23), the term associated with $A(k\rho)$ in (34) represents the diffracted wave which appears to arise from the edge; its dependence upon the wedge impedance function c_0 has already been discussed in connection with (15). The transition function $T(\rho, \phi + \phi')$ compensates for the divergent behavior of that portion of the diffracted wave amplitude which behaves like $1/(\pi - \phi - \phi')$ as $(\phi + \phi') \to \pi$.

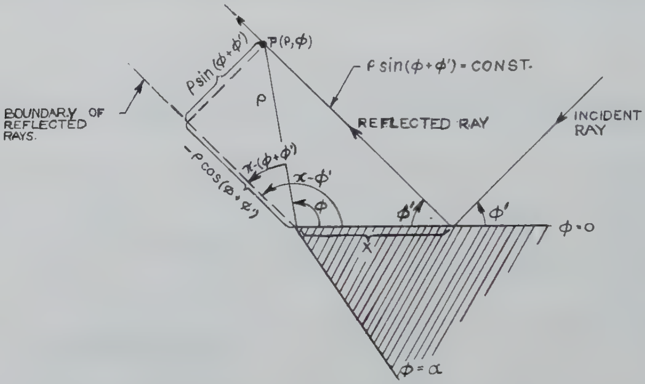

Fig. 6. Interpretation of geometrically reflected rays.

The first term on the right-hand side of (34) exists only when $\phi < (\pi - \phi')$; the exponential term $\exp[-(ik\rho\cos(\phi + \phi'))]$ permits its contribution to be identified as that from a ray which is reflected from the wedge face at $\phi = 0$ at the angle of incidence (see fig. 6). The amplitude of a reflected ray, given by

$$\Gamma_0[k\rho\sin(\phi + \phi')] = \frac{ic_0k\rho\sin(\phi + \phi') - 1}{ic_0k\rho\sin(\phi + \phi') + 1}, \tag{35}$$

is constant along the ray since the equation of a reflected ray is given by $\rho\sin(\phi + \phi') = \text{constant}$, as noted from fig. 6. The amplitude differs, however, for each ray so that the complex of reflected rays does not define a uniform plane wave. It is of interest to compare Γ_0 in (35) with the plane wave reflection coefficient $\bar{\Gamma}_0$ appropriate to an infinitely extended plane surface with constant impedance $\bar{z}_0$,

$$\bar{\Gamma}_0(\phi') = \frac{\bar{\gamma}\sin\phi' - 1}{\bar{\gamma}\sin\phi' + 1}, \tag{36}$$

where the constant $\bar{\gamma}$ is defined for the two polarizations as follows:

$$\bar{\gamma} = \bar{z}_0, \ \bar{z}_0 = \sqrt{\frac{\varepsilon}{\mu}}\, \hat{\bar{z}}_0, \ \text{for } E \text{ parallel to plane,} \tag{36a}$$

$$\bar{\gamma} = \frac{1}{\bar{z}_0}, \ \text{for } H \text{ parallel to plane.}$$

ϕ' is the angle of incidence measured away from the surface.

Along the surface $\phi = 0$, (35) can be written as

$$\Gamma_0(k\rho \sin \phi') = \frac{\gamma(x) \sin \phi' - 1}{\gamma(x) \sin \phi' + 1}, \ \gamma(x) = ikc_0 x, \ x = \rho \cos \phi. \tag{37}$$

x is the distance measured from the apex to the point at which the specularly reflected ray passing through $P(\rho, \phi)$ leaves the surface. Upon comparing (36), (36a), and (37), one notes that the amplitude of the reflected ray is the same as would be obtained for a uniform plane wave reflected from an infinite surface having a constant impedance identical to that at x. This conclusion is in agreement with predictions based on geometric-optical reasoning.

Contribution from $\Gamma_{\alpha} G_{\phi\infty}(\phi, 2\alpha - \phi')$. The contribution from the image source at $(2\alpha - \phi')$ in the infinitely extended angular region is given by $L_2(2\alpha - \phi' - \phi)$, where L_2 is taken from (34), provided that c_0 is replaced everywhere by c_α. The physical interpretation of the various contributions is the same as above, except that all considerations now involve the wedge face at $\phi = \alpha$.

§ 4. *Final result.* The asymptotic solution for all values of ϕ and ϕ' (except in the transition regions $\phi + \phi' \approx \pi$ and $2\alpha - (\phi + \phi') \approx \pi$) can now be written to $0(1/\sqrt{k\rho})$ for $\rho' \to \infty$, $k\rho \gg 1$, $\alpha > \pi$ as:

$$G(\underline{\rho}, \underline{\rho}') \sim \frac{i}{4} A(k\rho')[G_{\text{opt}}(\underline{\rho}, \phi') + G_{\text{diff}}(\underline{\rho}, \phi') + G_{\text{trans}}(\underline{\rho}, \phi')], \tag{38}$$

$$\begin{aligned} G_{\text{opt}} = {} & e^{-ik\rho \cos(\phi - \phi')} H(\pi - |\phi - \phi'|) + \\ & + \Gamma_0[k\rho \sin(\phi + \phi')]\, e^{-ik\rho \cos(\phi + \phi')} H(\pi - \phi - \phi') + \\ & + \Gamma_\alpha[k\rho \sin(2\alpha - \phi - \phi')]\, e^{-ik\rho \cos(2\alpha - \phi - \phi')} H[\pi - (2\alpha - \phi - \phi')], \end{aligned} \tag{38a}$$

$$G_{\text{diff}} = -4iI_0(\phi, \phi')\, A(k\rho), \tag{38b}$$

$$G_{\text{trans}} = -T(\rho, |\phi - \phi'|) - T(\rho, \phi + \phi') - T(\rho, 2\alpha - \phi - \phi'), \tag{38c}$$

where $A(x)$ is defined in (10). The diffracted wave function $I_0(\phi, \phi')$ has been shown to have the same functional form (as a function of ϕ, ϕ') for all geometric-optical domains. An integral representation for I_0 valid when $|\phi - \phi'| > \pi$ is given in (11). Thus, I_0 could be evaluated from (11) and the resulting function employed for all values of ϕ, ϕ'. G_{trans} in (38*c*) is significant only in the various transition regions. It affords a complete transition through the light-shadow boundary $|\phi - \phi'| = \pi$, but does not apply in the immediate vicinity of the reflected wave boundaries at $(\phi + \phi') = \pi$, $(2\alpha - \phi - \phi') = \pi$ (see remarks following (34)).

One verifies readily that the asymptotic solution in (38) satisfies to $0(1/\sqrt{k\rho})$ the required boundary condition $G = \mp c_{0,\alpha}(\partial G/\partial\phi)$ at $\phi = 0, \alpha$. Since G_ϕ satisfies this condition, one notes that for I_0 in (11)

$$I_0 = \mp c_{0,\alpha} \frac{dI_0}{d\phi}, \quad \phi = 0, \alpha. \tag{39}$$

For the geometric-optical term in (38*a*) one finds when $\phi' < \pi$,

$$\frac{1}{c_0} G_{\text{opt}} = - \frac{dG_{\text{opt}}}{d\phi} \left(1 - \frac{c_0 \cot \phi'}{ic_0 k\rho \sin \phi' + 1}\right)^{-1}, \quad \phi = 0, \tag{40}$$

and similarly for $\phi = \alpha$. Since $dG_{\text{opt}}/d\phi$ is $0(1)$ in $k\rho$, the geometric-optical contribution satisfies the boundary conditions at the wedge faces to $0(1/k\rho)$.

It is of interest to note that the asymptotic solution in (38) does not exhibit explicitly the presence of the surface wave discussed in [1]), which can propagate along the wedge face at $\phi = 0$ when $c_0 > 0$, or along the wedge fact at $\phi = \alpha$ when $c_\alpha > 0$. It is recalled, however (see (20) of [1])), that the surface wave varies like $1/\sqrt{k\rho}$ as $\rho \to \infty$ so that its effect in this case is indistinguishable from the diffracted field contribution.

An explicit evaluation of I_0 has been obtained in (15) for the special case $\Gamma_\alpha = 0$ where the wedge face at $\phi = \alpha$ is a perfect absorber for "angularly propagating waves". In this connection, we point out that I_0 in (11) can also be evaluated for the physically more significant special case wherein the wedge faces at $\phi = 0$ and $\phi = \alpha$ are purely reactive, with the reactance at $\phi = 0$ opposite in sign to that at $\phi = \alpha$, i.e., $c_0 = - c_\alpha > 0$. This implies via (3) that $\Gamma_0 \Gamma_\alpha = 1$ so that from (4)

$$G_\phi(\phi, \phi'; \mu^2) = G_\phi(\phi, \phi'; \mu^2)|_{\Gamma_0=\Gamma_\alpha=1} +$$
$$+ \left(\frac{1}{\Gamma_0} - 1\right) \sum_{n=1}^{\infty} G_{\phi\infty}(\phi, 2n\alpha - \phi') + (\Gamma_0 - 1) \sum_{n=0}^{\infty} G_{\phi\infty}(\phi, -2n\alpha - \phi'),$$
$$c_0 > 0. \quad (41)$$

Thus, G_ϕ can be expressed in this case in terms of the result for a perfectly reflecting wedge ($\Gamma_0 = \Gamma_\alpha = 1$) plus correction terms which involve only the first power of Γ_0 or $(1/\Gamma_0)$. Upon substituting (41) into (11) one obtains:

$$I_0(\phi, \phi') = I_0(\phi, \phi')|_{\Gamma_0=\Gamma_\alpha=1} + \frac{1}{4c_0} \sum_{n=0}^{\infty} \{B(2n\alpha + \pi + \varphi, c_0) -$$
$$- B(2n\alpha - \pi + \varphi, c_0) + B[2(n+1)\alpha - \pi - \varphi, -c_0] -$$
$$- B[2(n+1)\alpha + \pi - \varphi, -c_0]\}, \quad \varphi = \phi + \phi', \quad (42)$$

where the first term on the right-hand side of (42) is the known expression for the perfectly reflecting wedge [13])

$$I_0(\phi, \phi')|_{\Gamma_0=\Gamma_\alpha=1} = -\frac{\pi}{8\alpha} \sin\frac{\pi^2}{\alpha} \cdot$$
$$\cdot \left[\frac{1}{\cos\frac{\pi^2}{\alpha} - \cos\frac{\pi}{\alpha}(\phi - \phi')} + \frac{1}{\cos\frac{\pi^2}{\alpha} - \cos\frac{\pi}{\alpha}(\phi + \phi')}\right]^{*)}, \quad (42a)$$

and the remaining terms are corrections involving the exponential integral in (15*a*).

Acknowledgment The author is currently on a leave of absence from the Microwave Research Institute of the Polytechnic Institute of Brooklyn, where this work was performed under Subcontract 96 of Contract No. AF–19(122)–458 for the Lincoln Laboratory of the Massachusetts Institute of Technology.

Received 30th November, 1960.

---

*) Substitution of (4), with $\Gamma_0 = \Gamma_\alpha = 1$, into (11) yields for I_0 a series representation which can be summed into the closed form (42*a*) via the formulas

$$\cot x = \frac{1}{x} + 2x \sum_{n=1}^{\infty} \frac{1}{x^2 - (n\pi)^2}, \quad \text{and} \quad \cot\frac{x+y}{2} + \cot\frac{x-y}{2} = \frac{2\sin x}{\cos y - \cos x}.$$

REFERENCES

1) Felsen, L. B., Electromagnetic Properties of Wedge and Cone Surfaces with a Linearly Varying Surface Impedance, IRE Transactions PGAP, Vol. AP–7, Dec. 1959 (Special Supplement).

2) Felsen, L. B., Radiation from a Tapered Surface Wave Antenna, IRE Transactions PGAP, November 1960.

3) Keller, J. B., A Geometrical Theory of Diffraction, Calculus of Variations and its Applications, Proc. Symp. on Appl. Math., Vol. 8, 27–52, McGraw-Hill Book Co., New York, 1958.
Keller, J. B., J. Appl. Phys. **28** (1957); also, J. Appl. Phys. **29** (1958) 744.
Keller, J. B., Back-scattering from a finite cone, Rept. EM–127, Inst. Math. Sci., NYU 1959.
Keller, J. B. and B. Levy, Commun. Pure Appl. Math. **12** (1959).
Keller, J. B. and B. Levy, Diffraction by a spheroid, Rept. EM–130, Inst. Math. Sci., NYU 1959.
Keller, J. B. and B. Levy, Decay exponents and diffraction coefficients for surface waves on surfaces of nonconstant curvature, IRE Trans. AP–7, 1959, p. 852.

4) Felsen, L. B., Diffraction by an Imperfectly Conducting Wedge, Proc. of the McGill Symp. on Microwave Optics held at McGill University, Canada, June 1953.

5) Oberhettinger, F., J. Res. Nat. Bur. Stand., Wash. **61** (1958).

6) Cf. R. W. P. King and T. T. Wu, The Scattering and Diffraction of Waves, Harvard U. Press, Cambridge, Mass., 1959.

7) Clemmow, P. C., Infinite Integral Transforms in Diffraction Theory, IRE Trans. AP–7, 1959 (Special Supplement).

8) See also J. B. Keller, R. M. Lewis, B. D. Seckler, Commun. Pure App. Math. **9** (1956) 211.

9) Erdelyi, A., Higher Transcendental Functions, Bateman Manuscript Project, McGraw-Hill Book Co., New York, 1953, Vol. II, p. 143–147.

10) Sommerfeld, A., Partial Differential Equations in Physics, Academic Press, New York, 1949, p. 89.

11) Cf. B. L. van der Waerden, Appl. Sci. Res., B2 (1951) 191.

12) A tabulation of the Fresnel integral function $F(*)$ is given, for example, in E. Jahnke and F. Emde, Tables of Functions, Dover Publications, New York, 1945, p. 35–40.

13) Sommerfeld, A., Ch. 20 in Die Differential- und Integralgleichungen der Mechanik und Physik, Vieweg and Sons, Braunschweig, Germany, 1935. Edited by P. Frank and R. v. Mises.

Appl. sci. Res. Section B, Vol. 9

SOME DIFFRACTION PATTERNS OF AN ABSORBING HALF-PLANE *)

by CHESTER J. MARCINKOWSKI

Microwave Research Institute, Polytechnic Institute of Brooklyn, New York, U.S.A.

Summary

Far-field diffraction patterns are presented for the two-dimensional electromagnetic problem of plane wave scattering by a half-plane with a constant surface impedance. Previous results have been mainly concerned with a small surface impedance . In contrast with this, our diffraction patterns have been computed for the relatively arbitrary impedance of a half-plane which acts like a black screen for a prescribed angle of plane wave incidence. Such a half-plane may produce no reflected plane wave. Numerical calculations for the far fields show that the back-scattered fields are more noticeably influenced by the surface impedance than the forward-scattered fields. Nulls are found in the back-scattered fields. This type of black screen produces approximately the same scattering as the Sommerfeld black screen. Simple qualitative estimates of the diffracted far fields may be made without elaborate calculations.

§ 1. *Introduction.* The two-dimensional electromagnetic problem of diffraction by a dissipative half-plane with a constant surface impedance has been the subject of extensive investigations. Complete solutions for plane wave scattering were obtained by Senior [1]) in 1952 by means of the Wiener-Hopf technique. These results were later extended by Senior [2]) to solutions of the three-dimensional electromagnetic problem. It is well known that similar mathematical problems also occur in the coastal refraction of electromagnetic waves. A large amount of work has been carried out in this field particularly by the Russian school of investigators who include V. A. Fock [3]) and his associates. They have worked out many details of this basic problem, including the Wiener-Hopf solutions. The two-dimensional electromagnetic problem of plane wave scattering by a constant impedance wedge of arbitrary angle was solved by Senior [4]) and Williams [5]). For the special case of a wedge of zero angle the solutions of Senior and Williams simplify to those of the constant impedance half-plane.

---

*) Submitted in partial fulfillment of the requirements for the Ph. D. degree at New York University. Sponsored by Air Force Cambridge Research Laboratories, ARDC, under Contract AF—19 (604)—4143.

Previous investigators have appeared to consider their constant impedance, half-plane solutions primarily as approximations to a metallic half-plane with a small surface impedance. In contrast with this point of view we consider an absorbing half-plane with a relatively arbitrary, constant surface impedance. In particular we investigate some of the scattering properties of a half-plane which acts like one type of black screen with a constant surface impedance [6]). For a prescribed angle of plane wave incidence this type of half-plane produces no reflected plane wave. The three-dimensional electromagnetic problem of plane wave scattering by a black screen of this kind located on one side of a perfectly conducting right-angled wedge was solved by Karal and Karp [7]). Another type of black screen is a half-plane which is perfectly absorbing for "angularly propagating waves" incident upon it; this is Sommerfeld's black screen [8]). The surface impedance of such a half-plane is a function of position and its physical realizability is open to question. Nevertheless, the diffraction pattern of such a black screen is very simple to obtain [9]) so that it is easy to compare the nature of the scattering produced by the two different kinds of black screens.

It is characteristic of the more difficult Wiener-Hopf problems that they lead to factorized functions whose explicit evaluation requires the integration of a known function. For the constant impedance half-plane Senior [1]) obtained an explicit evaluation of the integral in question. The Russian investigators studying problems in coastal refraction have made use of a much simpler solution obtained by Grinberg and Fock [3]) with applications primarily to low impedance surfaces. We make use of the solution obtained by Grinberg and Fock and we extend the range of all parameters in their solution into the desired regions by analytic continuation. As a result of this procedure we obtain reasonably simple, explicit expressions for the two-dimensional electromagnetic problem of plane wave diffraction by a half-plane with a relatively arbitrary, constant impedance. In these expressions the surface impedance is described by means of an "angle of perfect absorption". This is defined as the angle at which an incident plane wave produces no reflected plane wave. This procedure has not only a simple geometrical significance but it also describes the half-plane impedance in a form which is useful and convenient for a physical interpretation of the diffraction patterns. Consequently, it is possible to describe the far-field diffraction patterns in terms of three simple dimensionless parameters: the angles of incidence, observation and perfect absorption.

The diffracted far-field patterns for several representative angles of incidence and perfect absorption will be described. It was found that the back-scattered fields are appreciably influenced by the surface impedance; the forward-scattered fields are quite insensitive to the nature of the surface impedance, especially in the shadow region. The Sommerfeld black screen and the half-plane which produces no reflected plane wave (the "perfectly absorbing" half-plane) both give approximately the same diffraction patterns. An interesting feature is the existence of nulls which occur only in the back-scattered fields. The locus of these nulls is given by a simple equation. The results obtained allow us to interpret the asymmetric diffraction patterns for the absorbing half-plane as a kind of distortion of the symmetric diffraction patterns for a perfectly reflecting half-plane. In this distortion the locus of the nulls is shifted and the scattering amplitude is correspondingly distorted. The main properties of the diffracted far-fields may be predicted in a qualitative manner by means of relatively simple calculations.

§ 2. *The far-field solutions.* In this section the asymptotic far-field solutions will be given for the two-dimensional electromagnetic problem of plane wave scattering by an absorbing half-plane with an arbitrarily prescribed, constant impedance. A complete transmission line formulation and Wiener-Hopf solutions have been described elsewhere [6]). The geometry of the problem is illustrated in fig. 1. A plane wave is incident on the impedance half-plane at angle ϕ_i while the field is observed at a point P with the polar coordinates ρ, ϕ where $-\pi/2 < \phi < 3\pi/2$. The angle at which an incident plane wave produces no reflected plane wave is denoted by ϕ_a, the angle of "perfect absorption". All fields are independent of the y coordinate. Both kinds of polarizations are considered in which either the total electric or total magnetic field may be along the y direction parallel to the edge of the half-plane. The rationalized MKS system of units and a suppressed time variation $\exp j\omega t$ are employed. For each polarization the surface impedance Z of the absorbing half-plane is defined by the relations

$$Z = \frac{\omega\mu}{k \cos \phi_a}$$

or (1)

$$Z = \frac{k}{\omega\varepsilon} \cos \phi_a$$

if the total electric or magnetic field respectively is parallel to the edge of the half-plane. The propagation constant of the medium is $k = \omega(\mu\varepsilon)^{\frac{1}{2}}$ where ω is the angular frequency and μ and ε are the permeability and permittivity of the medium. In this way the impedance is normalized and specified in terms of a dimensionless parameter ϕ_a which has a simple and interesting physical significance. If the angle of incidence $\phi_i = \phi_a$, then a plane wave incident on an infinite plane surface with impedance Z is perfectly absorbed since no reflected wave of any kind is produced. If the same plane wave is incident on a half-plane with the same surface impedance, then it is "perfectly absorbed" in the sense that no reflected plane wave is produced, although a scattered, cylindrical wave is created. Williams[5]) specifies the surface impedance in terms of an angle α which is equivalent to ϕ_a, but he does not introduce a physical interpretation of this angle as described here.

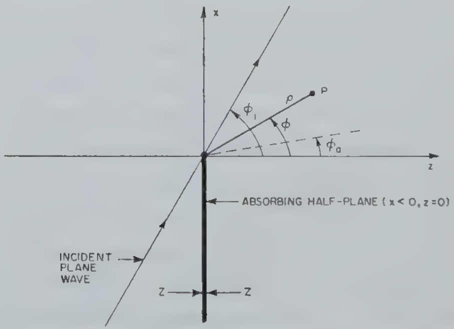

Fig. 1. The geometry of the constant impedance half-plane.

Our procedure allows us to specify the far-field scattering patterns in a physically significant manner for both types of polarization in terms of three similar, dimensionless parameters: the angle of incidence ϕ_i, the angle of observation ϕ and the angle of perfect absorption ϕ_a.

The Wiener-Hopf solutions provide the expected geometric optic fields (the incident and reflected plane waves) and a remaining diffracted field. This latter field may be evaluated by a standard saddle point evaluation to obtain the desired far-field behaviour ($k\rho \to \infty$). If the observation point $\mathrm{P}(\rho, \phi)$ in the far-field is sufficiently far from the shadow-lit boundaries of the incident and reflected plane waves, then a pole singularity is sufficiently far from the saddle point. Under these simpler conditions the y component of the field for either polarization is given by

$$F(\rho, \phi, \phi_i, \phi_a) \simeq A(\phi, \phi_i, \phi_a)\, f(\rho),$$

where

$$f(\rho) = j\left(\frac{2}{\pi k\rho}\right)^{\frac{1}{2}} e^{-j(k\rho - (\pi/4))} \tag{2}$$

and

$$A(\phi, \phi_i, \phi_a) = \frac{\cos\phi_i\, e^{b(\theta)} \left(\dfrac{\sin\phi_i + \sin\phi_a}{\sin\theta + \sin\phi_a}\right)^{\frac{1}{2}}}{2(\cos\phi_i + \cos\phi_a)(\sin\theta - \sin\phi_i)} \cdot$$

$$\cdot \left[\varepsilon(z)\cos\theta + \cos\phi_a \left(\frac{1 + \sin\theta}{1 + \sin\phi_i}\right)^{\frac{1}{2}}\right], \tag{3}$$

$$b(\theta) = \frac{1}{2\pi}\int_{u_1}^{u_2} \frac{u}{\sin u}\, \mathrm{d}u + \frac{1}{2\pi}\int_{u_3}^{u_4} \frac{u}{\sin u}\, \mathrm{d}u,$$

$$u_1 = \phi_i + \phi_a - \pi, \qquad \theta = \phi \text{ if } -\pi/2 < \phi \leq \pi/2$$

$$u_2 = \theta + \phi_a - \pi, \qquad = \pi - \phi \text{ if } \pi/2 \leq \phi < 3\pi/2,$$

$$u_3 = \theta - \phi_a, \qquad \varepsilon(z) = \pm 1 \text{ if } z \gtrless 0,$$

$$u_4 = \phi_i - \phi_a, \qquad 0 < (\phi_i \text{ or } \phi_a) < \pi/2.$$

The apparent discontinuity created by the $\varepsilon(z)$ term vanishes since $\cos\theta$ vanishes for $z = 0$. Moreover, to this order of approximation the field on the imperfectly reflecting half-plane vanishes. The next higher order saddle point approximation is needed to obtain non-vanishing (and discontinuous) fields on the imperfectly reflecting half-plane. Under certain conditions a pole singularity in the plane of integration at $-\pi + \phi_a$ will approach the saddle point if $\theta \to -\frac{1}{2}\pi$ and $\phi_a \to \frac{1}{2}\pi$. This corresponds to a point of observation near the absorbing half-plane when the latter has a surface impedance which absorbs perfectly a plane wave at grazing incidence. Under these rather special conditions the results of (2) need to be modified. However, this correction is negligible for all values of surface impedance and angle of observation which we will consider.

§ 3. *The diffraction patterns.* To ascertain the properties of the far-fields the amplitude of the angular pattern function $|A(\phi, \phi_i, \phi_a)|$ given in (3) has been calculated as a function of ϕ, the angle of observation. To cover a representative range of angles of plane wave incidence, the angles $\phi_i = 0°$, 45° and 80° were chosen. For each value of ϕ_i the representative angles of perfect absorption, $\phi_a = 10°$, 45°, 80° and 90° were chosen. The resulting far-field diffraction patterns are shown in figs 2, 3 and 4. For each ϕ_i in each of these figures there are four curves, one for each of the four values of ϕ_a. One of these four curves ($\phi_a = 90°$) is the well-known scattering

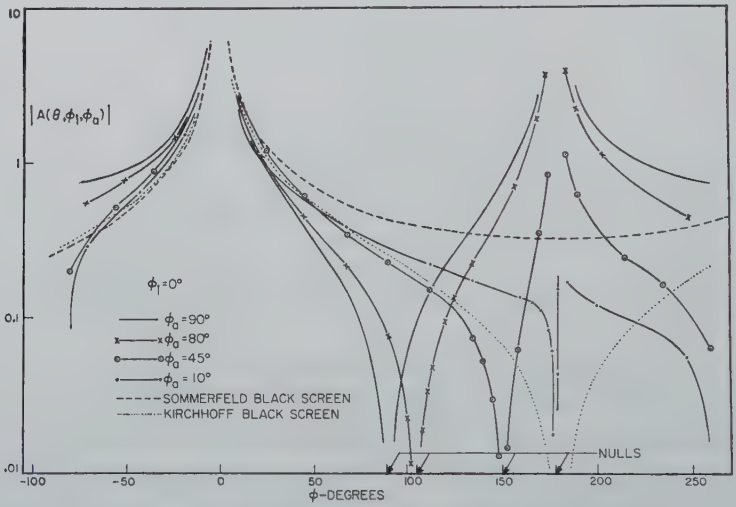

Fig. 2. Diffraction patterns for different absorbing half-planes. ($\phi_1 = 0°$)

pattern for a perfectly reflecting half-plane when the magnetic field is polarized parallel to the edge of the half-plane. In addition, two more curves have been added to each figure. The first added curve (the dashed line) is the scattering pattern for a half-plane which is perfectly absorbing for "angular propagating modes"; this is Sommerfeld's black screen. Its far-field angular pattern function is given by 9)

$$A(\phi, \phi_i) = \frac{\pi}{\pi^2 - (\pi + \phi_i - \phi)^2}\,. \tag{4}$$

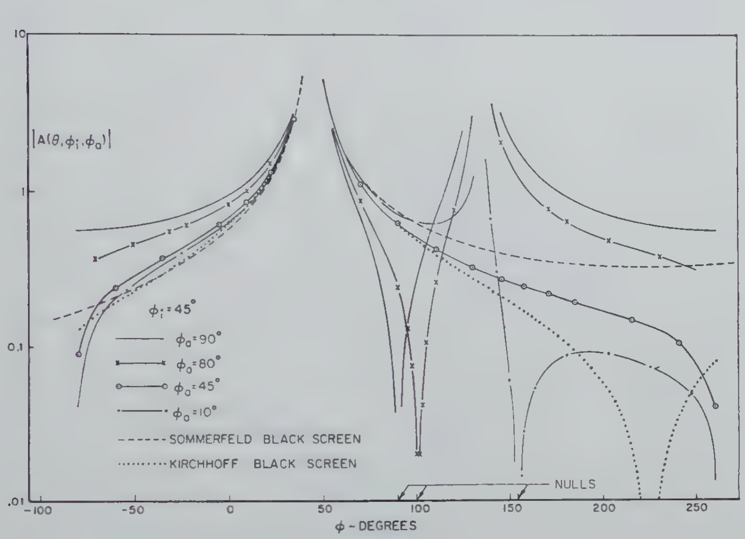

Fig. 3. Diffraction patterns for different absorbing half-planes. ($\phi_i = 45°$)

The second added curve in each figure (the dotted line) is the scattering pattern for the well-known Kirchhoff black screen. For this type of black screen it is assumed that the tangential electric and magnetic fields vanish on the absorbing half-plane while the aperture field is assumed to be the incident plane wave. The resulting far-field angular pattern function is given by 10)

$$A(\phi, \phi_i) = -\tfrac{1}{4}\cot\left(\frac{\phi_i - \phi}{2}\right). \tag{5}$$

The scattered fields contain the usual two shadow-lit boundaries for the incident and reflected plane waves at $\phi = \phi_i$ and $\phi = \pi - \phi_i$

except when $\phi_i = \phi_a$ in figs 3 and 4. For these latter two curves the reflected plane wave is absent ("perfect absorption"), and consequently the scattered field is finite and smoothly continuous across the non-existent shadow-lit boundary. As mentioned previously the scattered field amplitude tends to vanish as the observation angle ϕ approaches the surface of the imperfectly conducting half-plane. These factors serve to establish the general behaviour of the fields at the shadow-lit boundaries and the half-plane surface boundaries.

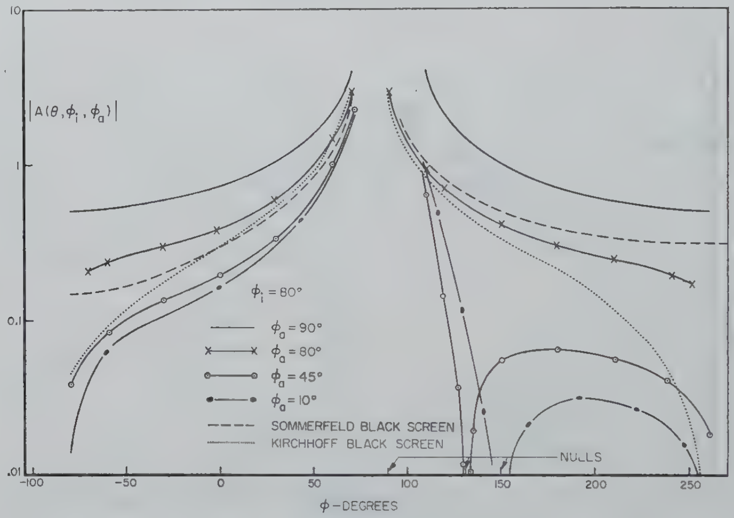

Fig. 4. Diffraction patterns for different absorbing half-planes. ($\phi_i = 80°$)

An interesting general feature of these curves is the presence of nulls in the scattering pattern for certain angles of observation as indicated in figs 2, 3 and 4. The angular pattern function $A(\phi, \phi_i, \phi_a)$ given by (3) vanishes if the terms in the square brackets vanish. For the range of values for ϕ, ϕ_i and ϕ_a given in (3), these terms will vanish only if $z < 0$, that is if $\pi/2 < \phi < 3\pi/2$. Consequently, nulls occur only in the back-scattered fields and not in the forward-scattered fields. With this restriction on ϕ the locus of the nulls is given by

$$\sin \phi = 1 - \frac{\cos^2 \phi_a}{1 + \sin \phi_i}. \tag{6}$$

For the special condition $\phi_a = \phi_i$ when no reflected plane wave is present, (6) simplifies to $\phi = \pi - \phi_i$. The location of this zero coincides with the location of the pole singularity in $A(\phi, \phi_i, \phi_a)$ which gives rise to the geometric optic reflected plane wave. As a result, the reflected plane wave disappears for this special condition and the scattering pattern is a finite, smooth and continuous function of ϕ across the no longer existing shadow-lit boundary at $\phi = \pi - \phi_i$.

When the magnetic field is polarized parallel to the edge of the half-plane, then the half-plane is perfectly reflecting when $\phi_a = \pi/2$ as indicated by (1). Under these conditions the well known scattered far-fields of the perfectly reflecting half-plane for all angles of plane wave incidence are symmetric with respect to the half-plane and exhibit a null in the aperture half-plane at $\phi = \pi/2$. For the absorbing half-plane, figs 2, 3 and 4 indicate that these symmetry properties are approached as ϕ_a approaches $\pi/2$. Because of this property of the nulls, it is interesting and significant to interpret the asymmetric patterns of the absorbing half-plane as a kind of angular deformation or perturbation of the symmetric scattering patterns for the perfectly reflecting half-plane. This interpretation is valid for both kinds of polarization. Depending upon whether the electric or magnetic field is polarized parallel to the edge of the half-plane, we have a perturbation about a small admittance or a small impedance [$\phi_a = \pi/2$ in (1)].

A study of the scattering patterns in figs 2, 3 and 4 shows that the scattered fields are most sensitive to the surface impedance in the back-scattering direction ($\pi/2 < \phi < 3\pi/2$) and much less sensitive in the forward-scattering direction ($-\pi/2 < \phi < \pi/2$). The half-plane with a surface impedance $\phi_a = \phi_i$, which produces no reflected plane wave, produces the smoothest scattering patterns. It is interesting to find that this "perfectly absorbing" half-plane produces approximately the same amount of scattering as the half-plane which is perfectly absorbing for "angularly propagating modes". This latter half-plane is Sommerfeld's black screen. The calculations for this black screen obtained from (4) are much simpler than the corresponding calculations for the constant impedance half-plane obtained from (3). In view of these results it may be plausible to suppose that the Sommerfeld black screen might serve as a simple, approximate mathematical model for a "perfectly absorbing" half-plane.

From the discussion given it should be easy to see how we might often obtain a reasonably accurate picture of the scattering pattern without actually performing the detailed calculations. To set the general level of the scattered field amplitude we might use the simple scattering pattern for the Sommerfeld black screen. Since the scattering near the shadow-lit boundaries tends to be independent of the surface impedance, the general behaviour near these regions could be reasonably approximated. Near the half-plane surface the vanishing of the fields could be estimated. Any nulls in the scattering pattern could be located from (6). From all this information a scattering pattern function could be sketched which would exhibit the main properties of the diffracted field in a qualitative manner and which would not require elaborate calculations.

I am indebted to Professors N. Marcuvitz and L. B. Felsen for their general guidance of this work and their many discussions and suggestions, and to Mrs. Toni Lotito for calculations of the scattered fields.

Received 20th December, 1960.

REFERENCES

1) Senior, T. B. A., Proc. Roy. Soc. A**213** (1952) 436.
2) Senior, T. B. A., Appl. Sci. Res. B **8** (1959) 35.
3) Grinberg, G. A. and V. A. Fock, Investigations on the Propagation of Radio Waves, edited by B. A. Vvedenskii, vol. 2, p. 69, Academy of Sciences Press, Moscow-Leningrad, 1948.
4) Senior, T. B. A., Comm. Pure Appl. Math. **12** (1959) 337.
5) Williams, W. E., Proc. Roy. Soc. A **252** (1959) 376.
6) Marcinkowski, C. J., Diffraction by an Absorbing Half-Plane, Microwave Research Institute, Polytechnic Institute of Brooklyn, Research Report R-750–59, September 29, 1959.
7) Karal, F. and S. N. Karp, Institute of Mathematical Sciences, Division of Electromagnetic Research, New York University, Research Report EM-111, February 1959.
8) Frank, P. and R. v. Mises, Die Differential- und Integralgleichungen der Mechanik und Physik, second edition, Vol. 2, p. 814, F. Vieweg and Son, Braunschweig, Germany, 1935.
9) Felsen, L. B. and N. Marcuvitz, Microwave Research Institute, Polytechnic Institute of Brooklyn, Electrophysics Group Memo. No. 14, June 8, 1956.
10) Baker, B. B. and E. T. Copson, The Mathematical Theory of Huyghens' Principle, second edition, p. 84, Oxford University Press, London, 1950.

Appl. sci. Res. Section B, Vol. 9

LETTER TO THE EDITOR

A "Wonderstone" microwave cavity for electron spin resonance spectrometers

In our laboratory we use a 3-cm esr spectrometer with phase-sensitive detection (modulation frequency 1000 Hz). This spectrometer has been described in detail elsewhere [1]).

When using a brass TE_{011} cavity we noticed that, even in the absence of electron spin resonance, the detected signal practically always differs from zero. This signal is caused by the interaction between the static magnetic field and the Foucault-currents induced in the walls of the cavity by the alternating magnetic field. This interaction causes a slight vibration of the cavity in a 1000 Hz-rythm so that the resonance frequency changes in the same rythm and the detected signal may contain a 1000 Hz component. This component is liable to fluctuate as a result of variations in temperature, klystron frequency and mechanical influences. These fluctuations manifest themselves as apparent noise, especially in measurements taking a long time as a result of broad resonance lines and application of long RC-times.

To suppress this troublesome phenomenon, it is necessary to minimize the generation of the Foucault-currents, by making the conducting walls of the cavity as thin as possible without weakening them mechanically. This can be achieved either in the way outlined by Eisinger and Feher [2]), who, applying ENDOR technique, used a pyrex cavity coated with silver on the inside; or with the procedure suggested by Thompson *et al* [3]) who, for the construction of their cavities with a low thermal expansion coefficient used silver-coated ceramic materials. Upon some orientations, however, we found that, at least for our laboratory, neither the coating of glass with a silver layer ensuring good adherence even at high temperatures, nor the machining of ceramic materials is an easy matter.

A very easy solution however was obtained with the aid of the South-African "wonderstone" (mainly pyrophyllite), which had already been used before by other workers [4]) e.g. as an insulating material. The properties of "wonderstone" have been described by Nel *et al.*[5]). If one follows the supplier's instructions (Carters Ltd., London), the construction of a wonderstone-cavity with the aid of conventional machine tools is not more difficult then that of a brass cavity.

A section of a tunable wonderstone transmission TE_{011} cavity, made by us, is shown in the figure. The outer section is rectangular, so that there is sufficient material to screw the lids 1 and 2 and the brass waveguides 3 and 4 on to the cylindrical casing 5. The cavity can be tuned by raising or lowering disc 7 with the aid of screw 6. Parts 2 and 6 are made of brass.

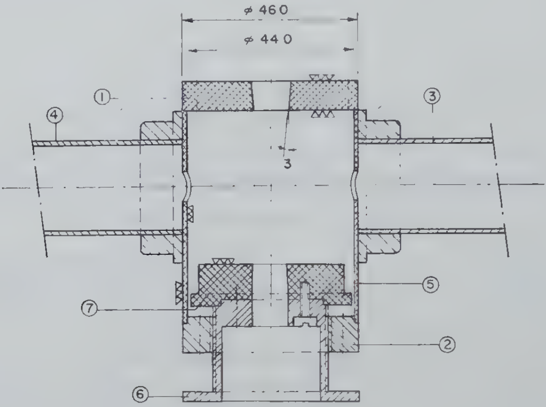

Fig. 1. Section of a transmission TE_{011} cavity. 1 and 2 lids, 3 and 4 brass waveguide, 5 cylindrical casing, 6 tuning screw, 7 disc.

The inside of the cavity is coated with Dupont's silver paste 6233. Without any polishing of the silver layer, the unloaded quality Q_u of such a cavity amounts to about 12000. The Q_u value of a brass cavity of the same design is about 10000, so that in this respect the wonderstone cavity is even better than a brass one. Moreover, the samples can be heated as easily in a wonderstone cavity as in a brass-cavity ^{1}).

With the aid of the cavity described we suceeded in improving the ratio between the signal and the apparent noise by a factor 5. More detailed information about the construction of the cavity will be given elsewhere ^{6}).

Received 6th December, 1960.

M. J. A. Bakker
J. Smidt
Centraal Laboratorium
Staatsmijnen in Limburg,
Geleen, Netherlands

REFERENCES

1) Smidt, J., Thesis Delft 1960.
2) Eisinger, J. and G. Feher, Phys. Rev. **109** (1958) 1172.
3) Thompson, M. C. Jr., F. E. Treathey and D. M. Waters, Rev. Sci. Instrum. **29** (1958) 865.
4) Carter, A. E., Br. J. Appl. Phys. **6** (1955) 326.
5) Nell, L. T., H. Jacobs, J. T. Allan and G. R. Bozzolí, Geol. Series Bull. No. 8, Union of S. Afr. Geol. Survey, 1937.
6) Bakker, M. J. A. and J. Smidt, Instrumentenbouw (to be published).

Appl. sci. Res. Section B, Vol. 9

SHEAR FLOW OF A VISCOUS INFINITELY ELECTRICALLY CONDUCTING FLUID PAST A POROUS FLAT PLATE IN THE PRESENCE OF A TRANSVERSE MAGNETIC FIELD

by A. S. GUPTA

Department of Applied Mathematics, Indian Institute of Technology, Kharagpur, India

Summary

An analysis is made for a uniform shear flow of an incompressible, viscous and perfectly electrically conducting fluid past a porous flat plate in the presence of a transverse magnetic field. It is shown that in the case of suction an asymptotic profile similar to that of Griffith and Meredith (for the flow of an incompressible viscous fluid past a porous plate) exists if the suction velocity is greater than the Alfvén velocity. In the case of injection, however, the asymptotic profile will exist if the Alfvén velocity is greater than the velocity of injection.

§ 1. *Introduction.* The flow of an incompressible viscous fluid past an infinite porous plate has been solved by Griffith and Meredith [1]). Sakurai [2]) has solved the same problem when there is a uniform vorticity in the main flow. The present note is an extension of the problem considered by Sakurai to the case of a perfectly electrically conducting fluid in the presence of a transverse magnetic field.

§ 2. *Basic equations and their solutions.* We take the x-axis along the plate (assumed to be non-conducting and non-magnetic) and the y-axis perpendicular to it. Since the plate is infinite, we can assume that all the physical variables are functions of y only.

The equation of continuity is

$$dv/dy = 0, \tag{1}$$

which gives

$$v = v_0, \tag{2}$$

v_0 being the constant normal velocity at the plate.

The equations of momentum are

$$\rho v_0 \frac{du}{dy} = -\frac{\partial p}{\partial x} + \mu \frac{d^2u}{dy^2} + \frac{\mu_e}{4\pi} H_y \frac{dH_x}{dy}, \tag{3}$$

$$O = -\frac{\partial p}{\partial y} - \frac{\mu_e}{4\pi} H_x \frac{dH_x}{dy}. \tag{4}$$

When $\sigma = \infty$, Maxwell's equations give

$$\text{curl } (\boldsymbol{q} \times \boldsymbol{H}) = 0, \tag{5}$$

$$\text{div } \boldsymbol{H} = 0. \tag{6}$$

Since H_x and H_y are functions of y only, (6) gives

$$H_y = \text{constant} = H_0, \tag{7}$$

and (5) gives

$$H_0 \frac{du}{dy} = v_0 \frac{dH_x}{dy}. \tag{8}$$

Since at $y = \infty$, $u = U_\infty + \Omega y$, we have from (8)

$$H_0 \Omega = v_0 \frac{dH_x}{dy}. \tag{9}$$

Equation (3) now gives

$$\frac{\partial p}{\partial x} = \alpha, \tag{10}$$

where

$$\alpha = \rho\Omega\left(\frac{\mu_e H_0{}^2}{4\pi\rho v_0} - v_0\right). \tag{11}$$

Using (7), (8) and (10) we get from (3)

$$\frac{d^2u}{dy^2} + \frac{\alpha}{\mu\Omega}\frac{du}{dy} - \frac{\alpha}{\mu} = 0. \tag{12}$$

The solution of (12) subject to $u = U_\infty + \Omega y$ at $y = \infty$ is

$$u = U_\infty + \Omega_y + c \exp\left(-\frac{\alpha y}{\mu\Omega}\right). \tag{13}$$

Since $u = 0$ at $y = 0$, the above equation gives

$$u = U_\infty + \Omega y - U_\infty \exp\left(-\frac{\alpha y}{\mu\Omega}\right). \tag{14}$$

In order that the above asymptotic solution may hold it is necessary that $\alpha > 0$. Hence we must have

$$\frac{\mu_e H_0^2}{4\pi v_0} > \rho v_0. \tag{15}$$

In the case of suction, $v_0 = -V$, $V > 0$, the above inequality becomes

$$V^2 > V^2_{\text{Alf}}, \tag{16}$$

where V_{Alf} stands for the Alfvén velocity $\sqrt{(\mu_e/4\pi\rho)}\, H_0$. In the case of injection, v_0 is positive, and the inequality can be written as

$$\frac{\mu_e H_0^2}{4\pi\rho} > v_0^2, \tag{17}$$

which shows that the Alfén velocity must be greater than the injection velocity.

In the absence of a magnetic field it has been shown by Sakurai that an asymptotic solution of the type (14) exists in the case of suction and not in the case of injection. However, the presence of a magnetic field in such a shear flow ensures the existence of asymptotic solutions of the type (14) both in the case of suction and injection provided the suction and injection velocity are respectively greater and less than the Alfvén velocity.

From (8) and (14) we get

$$\frac{dH_x}{dy} = \frac{H_0}{v_0}\left[\Omega + \frac{U_\infty \alpha}{\mu\Omega}\exp\left(-\frac{\alpha y}{\mu\Omega}\right)\right].$$

Integrating this equation and noting that $H_x = 0$ at $y = 0$ (the plate being non-magnetic and non-conducting), we get

$$H_x = \frac{H_0}{v_0}\left\{\Omega y + U_\infty\left[1 - \exp\left(-\frac{\alpha y}{\mu\Omega}\right)\right]\right\}. \tag{18}$$

Equation (10) gives on integration

$$p = \alpha x + F(y). \tag{19}$$

Substituting (19) in (4) and integrating we get

$$F(y) + \frac{\mu_e}{8\pi} H_x^2 = c_2.$$

Hence (19) gives the pressure distribution as

$$p = \alpha x - \frac{\mu_e}{8\pi} H_x{}^2 + c_2, \tag{20}$$

H_x being given by (18).

Received 21st January, 1961.

REFERENCES

1) Meredith, F. W. and A. A. Griffith, Modern Developments in Fluid Dynamics Oxford University Press, Vol. 2, 1938, pp. 534.
2) Sakurai, T., J. Aero. Sci. **24** (1957) 79.

Appl. sci. Res. Section B, Vol. 9

SOME PHENOMENA OCCURRING IN FLOATING BATTERY SYSTEMS

by M. v. MENTS

Research Council of Israel, Jerusalem, Israel.

Summary

The behaviour of a battery, its load and the supply system in floating condition is sometimes of a complicated nature. This applies in particular when the loading voltage is derived from a rectified a.c. supply which is not, or only partly, smoothed. In such a typical case it has been proved possible to express the equilibrium conditions of the system within a simple mathematical framework. The mathematical treatment and the results are elucidated and a numerical example met in practice is dealt with.

§ 1. *Introduction.* A battery continuously connected to a bus is said to float when the voltage of the charging line is slightly greater than the open-circuit voltage of the battery 1). There exists a great variety of examples where such a device is desirable. The conditions of the rectifier on the one side and of the load on the other put their stamp on the characteristics and the behaviour of the set-up.

It is a known fact that battery rectifiers need not be smoothed 2), and the same is true for the rectifier in a floating system. In the latter case, however, some interesting phenomena occur which may give rise to more complicated situations and difficulties than in the case of simple loading. The complications arise in particular when the floating batteries have to deliver current during a part of the cycle.

Such a case was encountered in realising the tension supply of the National Standard Clock in Israel 3). Because of the frequently occurring mains supply failures, use had to be made of a floating battery system for both high and low voltages. It transpired that equilibrium conditions were obtained after 5 or 10 hours only, and that there are situations where the floating voltage at the end is either lower (which means that the battery is slowly discharging) or higher than the prescribed values *).

In order to be able to handle the situation and to know in advance what values should be used for the several resistances and voltages of the circuit, a simple mathematical treatment of such a system was developed. The results proved to be very successful in promoting a better understanding of what happens in such systems. Some approximations and assumptions had to be made, so as not to complicate the calculations more than necessary. It has been verified, however, by practical observations that this mathematical treatment gives very reliable results.

§ 2. *The general set-up of a floating battery system.* A general scheme of a floating battery system is sketched in fig. 1. The internal resistance of the rectifier is given by R_{r1} and, as will be explained, may have to be completed by an extra one R_{r2}. The internal battery resistance R_{b1} will be greater by an amount R_{b2}, as caused by relay-contacts, wiring, etc. ^{4}). The load resistance R_{l1} may be greater by the amount R_{l2} for the same reasons, or by purposely adding resistance.

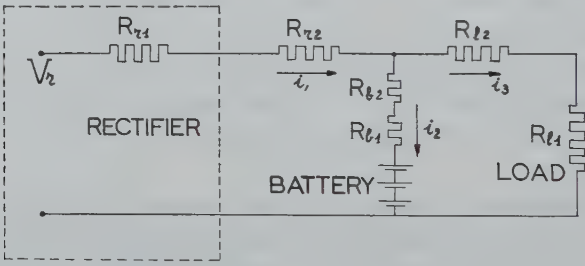

Fig. 1. General set-up of a floating battery system.

For a given time dependence of V_r, all these quantities are inter-related in some way, and some of them determine the value of the others. In most cases, part of the quantities may be fixed and invariable, right from the beginning (e.g. V_r, R_{r1}, R_{l1}), another part may have a prescribed value (say: the average load current $\bar{i}_3$ and the battery voltage V_b in floating position) and the rest (e.g. R_{r2})

---

*) See footnote in § 3.

may be chosen within certain limits. In the next section, the relations between the several quantities will be evaluated.

§ 3. *Mathematical treatment.* Let

$$\left.\begin{aligned} R_{r1} + R_{r2} &= R_r, \\ R_{b1} + R_{b2} &= R_b, \\ R_{l1} + R_{l2} &= R_l \end{aligned}\right\} \tag{1}$$

and further

$$R_r/R_l = r, \tag{2}$$

$$R_b/R_l = b, \tag{3}$$

$$\frac{R_rR_l + R_bR_l + R_rR_b}{R_l^2} = r + b + rb = s. \tag{4}$$

If it is ignored for the moment that i_1 cannot be negative in the case of an ideal rectifier, then the Kirchhoff relations

$$i_1 = i_2 + i_3, \tag{5}$$

$$V_r - i_1R_r - i_2R_b - V_b = 0, \tag{6}$$

$$i_3R_l - i_2R_b - V_b = 0 \tag{7}$$

should yield the currents in the several circuit branches. The result is found to be

$$i_1 = \frac{(1 + b)\, V_r - V_b}{sR_l}, \tag{8}$$

$$i_2 = \frac{V_r - (1 + r)\, V_b}{sR_l}, \tag{9}$$

$$i_3 = \frac{bV_r + rV_b}{sR_l}. \tag{10}$$

However, for an ideal rectifier, i_1 cannot be negative, so that (8), (9) and (10) only hold when $V_r > V_{cr}$ where from (8) the critical voltage V_{cr} is given by

$$V_{cr} = \frac{V_b}{1 + b}. \tag{11}$$

During that part of the cycle for which $V_r < V_{cr}$ there holds

$$i_1 = 0, \quad -i_2' = i_3' = \frac{V_b}{R_l(1 + b)}. \tag{12}$$

It will further be assumed that use is made of a full wave rectifier and that V_r is given by

$$V_r = |\hat{V}_r \sin \omega t|. \tag{13}$$

When no inductive or capacitive elements are present in the whole system, only the phenomena taking place during the time periods $0 \to t_1$ and $t_1 \to t_2$ will have to be studied (see fig. (2)), where

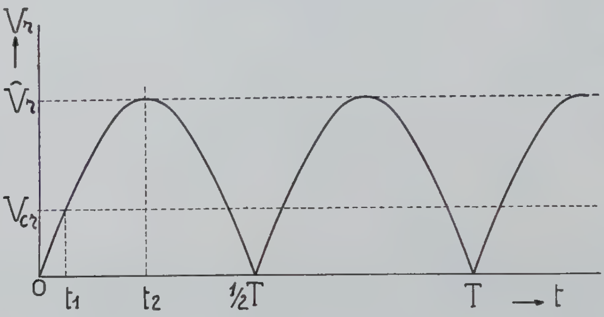

Fig. 2. Full wave rectification.

$$t_2 = \tfrac{1}{4}T = \pi/2\omega. \tag{14}$$

The time t_1 for which $V_r = V_{cr}$ is defined by

$$V_{cr} = \hat{V}_r \sin \omega t_1, \tag{15}$$

and using (11) it follows that

$$\sin \omega t_1 = \frac{V_b}{(1+b)\hat{V}_r}. \tag{16}$$

It will prove to be useful to define an auxiliary angle α by

$$\alpha = \pi/2 - \omega t_1. \tag{17}$$

Now it is assumed that the battery delivers the load current during that part of the cycle for which $V_r < V_{cr}$ and behaves then as if no rectifying system were present at all. As a result, the battery loses (between $t = 0$ and $t = t_1$) an amount of charge given by

$$Q_{\text{out}} = \int_0^{t_1} i_3' \, \mathrm{d}t = \frac{V_b}{\omega R_l(1+b)} \left(\frac{\pi}{2} - \alpha\right), \tag{18}$$

as can be easily verified with the help of (12) and (17).

The amount of charge, received by the battery during the second part of the cycle (between t_1 and t_2) is given by

$$Q_{\text{in}} = \int_{t_1}^{t_2} i_2 \, \mathrm{d}t = \int_{\pi/2-\alpha}^{\pi/2} \frac{\hat{V}_r \sin \omega t - V_b(1 + r)}{\omega s R_l} \, \mathrm{d}\omega t.$$

The result of the integration is

$$Q_{\text{in}} = \frac{\hat{V}_r \sin \alpha}{\omega s R_l} - \frac{V_b(1 + r)\alpha}{\omega s R_l}. \tag{19}$$

It is assumed that R_{b1} has the same and moreover constant value for both the time intervals $0 \to t_1$ and $t_1 \to t_2$. This is true only in first approximation, but as in any case $R_b \ll R_l$ in practically occurring systems, one need not bother about deviations. This will find its expression in (24).

The net charge per cycle is given by

$$Q_c = 4(Q_{\text{in}} - Q_{\text{out}})$$

and the net charge per second by

$$Q_s = \frac{1}{T} Q_c = \bar{i}_2. \tag{20}$$

Combination of (14), (18), (19) and (20) yields

$$\frac{\frac{1}{2}\pi(1 + b) R_l \bar{i}_2}{V_b} = \frac{\sin \alpha (1 + b) \hat{V}_r}{s V_b} - \frac{(1 + r)(1 + b)\alpha}{s} - \frac{\pi}{2} + \alpha. \tag{21}$$

By making use of (2)–(4), showing that

$$(1 + b)(1 + r) = s + 1,$$

and of (16) and (17), yielding

$$\frac{\hat{V}_r(1 + b)}{V_b} = \frac{1}{\cos \alpha},$$

it is easily seen that (21) goes over into

$$\tfrac{1}{2}\pi s(1 + \varepsilon) = \operatorname{tg} \alpha - \alpha \tag{22}$$

where ε is defined by

$$\varepsilon = \frac{(1 + b) R_l \bar{i}_2}{V_b}. \tag{23}$$

The value of ε is directly connected with the practical considerations that prescribe the value of V_b *).

Although no well-defined data can be found in literature with respect to the residue charging current $\bar{i}_2$, it has been proved by studying the instructions of the manufacturers that the charging current in floating condition is very small as compared with normal charge or load currents *). The electro-chemical processes occurring in this situation, where the battery tries to pull itself up to reach asymptotically the average bus voltage, play an important part of a very complicated nature.

In normal situations where $b \ll 1$ it follows from (23) that ε is given by $\varepsilon \approx \bar{i}_2/\bar{i}_3$, so

$$\varepsilon \ll 1. \tag{24}$$

(Only in cases where for some reasons $b \gg 1$ it follows that

$$\varepsilon \approx \bar{i}_2 R_b / V_b,$$

and it might be that the value of ε is then comparable with or even greater than unity). Inserting (24) into (22), yields

$$\tfrac{1}{2}\pi s \approx \operatorname{tg} \alpha - \alpha. \tag{25}$$

It seems that (25) (or eventually (23)) governs the relationship between all the quantities appearing in floating battery systems. This result will be demonstrated with an example, met during the installation of the National Standard Clock in Israel [3]). Here the following quantities were encountered for a low voltage supply:
$V_b = 6.5$ V (three cells; value given by manufacturer).
$R_b = 0.2\,\Omega$, $R_{l2} = 0.15\,\Omega$, $R_{l1} = 2.0\,\Omega$ (average, if $V_{l1} = 6.1$ V),
$\bar{i}_2 = 0.10$ A,
and use was made of a full wave selenium rectifier for which $\hat{V}_r = 15.7$ V, $R_{r1} = 0.70\,\Omega$, as measured with dummy loads.

Now the following values can easily be evaluated:

$$\begin{array}{ll}
b = 0.093 & \varepsilon = 0.036 \\
\sin \omega t_1 = 0.38 & s = 0.76 \\
\alpha = 1.18 \text{ radian} & r = 0.61 \\
\operatorname{tg} \alpha - \alpha = 1.26 & R_r = 1.31\,\Omega.
\end{array}$$

---

*) In practice, V_b varies between 2.15 and 2.20 volt, depending on the type of battery; the current $\bar{i}_2$ is of the order of 0.5 to 1.5% of the 8 hour rate of the battery.

As R_{r1} is 0.70 Ω, it easily follows from (1) that an extra resistance $R_{r2} = 0.61\ \Omega$ has to be added.

§ 4. *Conclusions.* With the help of the framework previously developed one can define the mutual relationship between the various parameters of the system and calculate their values.

It further enables us to investigate what happens in the case of slight variations of one or more of the values with respect to equilibrium values. Thus it is easily seen that

$$\frac{\partial V_b}{\partial R_r} = -\frac{\pi \hat{V}_r}{2R_l}(1+b)^2\left(\frac{\cos^2\alpha}{\sin\alpha}\right), \tag{26}$$

which means that one immediately knows how to change the added resistance R_{r2} in case of a drop or a rise in the observed battery voltage as measured at the terminals. Such events might occur e.g. by the ageing of a selenium rectifier. (In fact, it was experienced in the case of the example dealt with in the previous paragraph that the voltage dropped by 0.20 V after a couple of months. The situation could easily be restored by reducing the resistance R_{r2} by 0.10 Ω as follows from (26). A new equilibrium was obtained after a couple of hours, V_b having reached again the prescribed value of 6.5 V.)

Another practical application is to see whether the nature of (23) still offers enough freedom to cope with one or more other conditions. In the example treated it was e.g. highly desirable that the average load current $\bar{i}_3$ should remain the same in the case of disconnecting the battery. It can be shown that this condition implies

$$\frac{1}{\cos\alpha} = \frac{\pi}{2}(1+s)\left(1+\frac{b\varepsilon}{1+b}\right). \tag{27}$$

With the help of (22), (23) and (27) one is able to solve for all the quantities, to find amongst other things that $\hat{V}_r$ should have been chosen 30 V instead of 15.7 V, and $R_r = 4.1\ \Omega$.

The average load current would have been the same (3.05 A) with disconnected battery, whereas in the present case this current has a value of

$$i_3'' = \frac{2\,V_r}{\pi R_l(1+r)} = 2.90\ \text{A}$$

if one disconnects the battery.

Finally it is worthwhile investigating the ripple on the load voltage. Fig. 3 is drawn with the help of the results of (10), (12) and (13) and the values of the numerical example. The real time dependence could be verified by making use of an oscillograph and by measuring the voltage drops over the several resistances. The agreement between calculated and observed data provides a justification of the method as a whole.

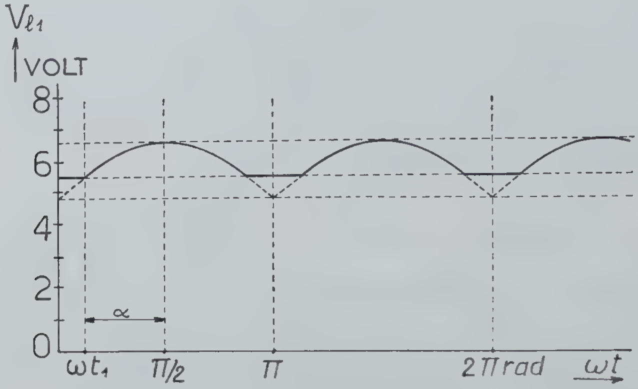

Fig. 3. The ripple on the load voltage; the figure is drawn according to the values of the numerical example.

Received 28th January, 1961.

REFERENCES

1) Wood Vinal, G., Storage Batteries, 4th ed., p. 256; New York, 1955.
2) Id. page 274.
3) Ments, M. v., Amer. J. Phys. **24** (1956) 489.
4) Willihnganz, E. and P. Rohner, Elect. Engng **78** (1959) 922.

Appl. sci. Res. Section B, Vol. **9**

AXISYMMETRIC STAGNATION POINT FLOW IN MAGNETOHYDRODYNAMICS

by W. I. AXFORD

Defence Research Telecommunications Establishment Ottawa, Canada *)

Summary

This paper contains a theoretical treatment of the axisymmetric stagnation point problem in magnetohydrodynamics. Two distinct arrangements of the magnetic field are considered, with the lines of force lying in the plane of, and perpendicular to the streamlines, respectively. The boundary conditions are examined carefully and the solutions are completed by joining them to meaningful distributions of magnetic field in the solid region. Exact solutions can be obtained by numerical methods, but it is more illuminating to consider approximations valid for very large and very small diffusion numbers (ratio of kinematic viscosity to magnetic diffusivity). Distinct boundary layers of current and vorticity occur in these limiting cases, which can be treated separately. For flows with the first arrangement of the magnetic field, and in which the field does not vanish at infinity, it is deduced that the solution refers to a forward stagnation point when the Alfvén number is less than unity, and to a rear stagnation point when the Alfvén number exceeds unity. An interesting choking effect is found in flows with the second arrangement of the magnetic field when the diffusion number is small, and the Alfvén number exceeds unity; it is believed that this effect could be demonstrated in the laboratory.

§ 1. *Introduction.* A number of papers have been written in the past few years on the subject of magnetohydrodynamic boundary layers. Most attention has been paid to the case of weakly conducting fluids, with the aim of predicting the effects that may be found in aeronautical situations, although other limiting cases have also been considered. In the present paper we hope to clarify some of the more general aspects of the subject without emphasizing particular numerical results. The problem we shall consider is that of axi-symmetric stagnation point flow of an incompressible, viscous, electrically conducting fluid in the presence of a magnetic field; this problem has the advantage that exact (numerical) solutions can be found if necessary to compare with approximate solutions. The term 'boundary layer' is used in a relative sense in this context and does not presuppose the existence of large Reynolds numbers.

---

*) Work carried out at Cambridge, England. The author is a member of the New Zealand Scientific Defence Corps.

Several authors have considered the stagnation point problem in magnetohydrodynamics, both for the two-dimensional and axi-symmetric cases, the first being Michael[1]) who examined the current layer in the two dimensional case with viscosity neglected. Michael's solution demonstrates the manner in which joint convection and diffusion of the lines of force produces a boundary layer of current, but as the existence of similarity solutions was not recognized by Michael, mathematical difficulties forced him to consider only the case of vanishingly weak magnetic field. Similarity solutions of the two-dimensional problem were examined by Neuringer and McIlroy[2]), whose methods, however, were questionable. This work was criticized by Hess[3]), but his paper did not succeed in reducing the confusion to any great extent.

The impression was given in Neuringer and McIlroy's work that their solution is exact, leading Rossow[4]) to believe that the close agreement with his approximate solution confirmed the validity of the approximations. However, as pointed out by Hess, the Rossow approximations were made by Neuringer and McIlroy in a hidden manner and the agreement of the solutions was to be expected. Rossow's boundary layer equation[5]) should be used with caution, for although it gives correct results in some cases[6]), there are other cases in which a careless treatment leads to results that are meaningless in the sense that they cannot be related directly to any flow problem. This is exemplified in the papers by Neuringer and McIlroy and Rossow[4]), where the behaviour of the magnetic field and the boundary conditions it must satisfy are not considered in any detail; it is not surprising then that we find that the results obtained by these writers are not particularly relevant to aeronautical situations (Hess). It is true that for a weakly conducting fluid, induced fields can be neglected in the viscous boundary layer, but this does not imply that induced fields can be neglected entirely as the field may interact strongly with the flow elsewhere, causing the field in the boundary layer (and within the boundary as well) to be distorted so that it cannot be specified in an *a priori* manner. The correct method of attacking the problem is given in this paper; it has also been given by Meyer [7]), who has obtained some numerical results. Further numerical results have been given by Poots and Sowerby [19]).

In cases where a shockwave occurs a short distance upstream of the stagnation point, and the fluid is electrically conducting only between the shock and the surface of the body, induced fields can be neglected if the magnetic Reynolds number based on the stand-off distance is small. Several authors have considered problems of this type, notably Meyer [8]), Kakutani [9]) and Oguchi [10]).

In contrast to the papers referred to so far, which treat only the case of weakly conducting fluids, the present paper treats both limits of very large and very small electrical conductivity. Two distinct arrangements of the magnetic field are considered; in the first arrangement the lines of force lie in planes which intersect the axis of symmetry, while in the second arrangement (which has not been considered before) the lines of force are circles and result from an applied axial current. The Alfvén (S) and diffusion *) (ε) numbers are found to be the most important parameters in the problem. For small diffusion numbers the region of flow in which diffusion of the lines of force (current layers) occurs is wider than the viscous boundary layer by a factor $O(\varepsilon^{-\frac{1}{2}})$, whereas for large diffusion numbers the viscous boundary layer is wider than the current layer by a factor $O(\varepsilon^{\frac{1}{3}})$. An interesting effect is found to occur in flows with the first arrangement of the magnetic field when the diffusion number is very large; whereas solutions for only the forward stagnation point are possible in ordinary hydrodynamics, the solution in the present example refers to a forward stagnation point when the Alfvén number is less than unity, and to a rear stagnation point when the Alfvén number exceeds unity. It is believed that the same effect occurs when the diffusion number is small, but confirmation from numerical solutions of the equations is required. A similar effect was found by Carrier and Greenspan [12]) in their analysis of the flat plate boundary layer problem. In flows with the second arrangement of the magnetic field, 'choking' occurs when the Alfvén number approaches unity and the diffusion number is very small; it is suggested that a laboratory demonstration of this result may be possible.

---

*) The term "diffusion number" is used throughout this paper to denote the ratio of kinematic viscosity to magnetic diffusivity. It seens to have been Batchelor [11]) who first skowed the significance of this quantity in magnetohydrodynamics. Sooner or later the quantity (magnetic diffusity/thermal diffusivity) must occur in the literature, and so, to avoid confusion it is suggested that the term "magnetic Prandtl number" should not be used.

It should be noted that the technique of separating the current layer and the viscous boundary layer, when the diffusion number is both very large and very small, cannot in general be regarded as forming a first approximation for a series solution in ascending or descending powers of ε, although one further iteration may be possible. However solutions can always be obtained in the form of a series in ascending powers of S; when $S = 0$, the solution for the velocity field is that obtained by Homann [13]), and the structure of the current layer is similar to that of a thermal boundary layer in the absence of buoyancy forces [14]).

Previously, many writers have ignored the details of the magnetic field in the solid regions, usually stating that a distribution of surface currents can always be found so that the conditions at the boundary are satisfied. In the author's opinion, a problem of this type should always be completed by joining the solution in the fluid to a suitable solution for the solid region [15]), otherwise the feasibility of the problem, as well as its relevance to any physical situation, may be in doubt. The solutions given here do not depend upon whether the solid is electrically conducting or not, and in particular they represent the steady state in all cases for which the conductivity of the solid is finite. Some authors (notably Michael) have made the assumption that the solid is a perfect conductor, but this is hardly reasonable for real materials in steady flow problems unless a superconductor is involved. For example, a rough calculation shows that any distortion of the magnetic field at the boundary of a solid copper body penetrates a distance of 10 centimetres in a time of about 2 seconds, which is not long in engineering contexts, except perhaps in shock tubes.

§ 2. *Stagnation point flow with no azimuthal magnetic field.* When there is axial symmetry, it is convenient to use cylindrical polar coordinates (r, θ, z) such that the stagnation point is at the origin and the regions $z > 0$ and $z < 0$ are occupied by fluid and solid material of uniform composition, respectively. The equations of magnetohydrodynamics in these coordinates have been given by Yih [16]) and others; for brevity we simply note that the solution of these equations for stagnation point flow, when the velocity and magnetic induction vectors have the forms (u, O, w) and (B_r, O, B_z) and there is axial symmetry $(\partial/\partial\theta \equiv 0)$, is

$$\psi = Ur^2\sqrt{(\kappa/U)}\, f(\phi),\quad A = Br^2\sqrt{(\kappa/U)}\, g(\phi). \tag{2.1}$$

Here ψ is a stream function and A the non-zero component of the magnetic vector potential, such that

$$u = \frac{1}{r}\frac{\partial\psi}{\partial z},\ w = -\frac{1}{r}\frac{\partial\psi}{\partial r},\quad B_r = \frac{1}{r}\frac{\partial A}{\partial z},\ B_z = -\frac{1}{r}\frac{\partial A}{\partial r}; \tag{2.2}$$

the independent variable is defined to be

$$\phi = \sqrt{(U/\kappa)}z, \tag{2.3}$$

and the constants U and B have the dimensions (velocity/length) and (magnetic induction/length) respectively, while κ has the dimensions of a diffusivity.

The pressure p has the form

$$p = p_0 - \tfrac{1}{2}\rho U^2 r^2 p_1(\phi) - 2\rho U\kappa p_2(\phi), \tag{2.4}$$

where ρ is the density of the fluid and p_0 is a constant. The functions $f(\phi)$, $g(\phi)$, $p_1(\phi)$ and $p_2(\phi)$ satisfy the following ordinary differential equations:

$$\frac{\nu}{\kappa} f''' + 2ff'' - f'^2 + p_1 = 2Sgg'', \tag{2.5}$$

$$\frac{\eta}{\kappa} g'' = 2gf' - 2fg', \tag{2.6}$$

$$p_1' = S(g'^2)', \tag{2.7}$$

$$p'_2 = (f^2)' + \frac{\nu}{\kappa} f'', \tag{2.8}$$

where primes denote differentiations with respect to ϕ, ν is the kinematic viscosity and η the magnetic diffusivity of the fluid, $S \equiv B^2/4\pi\mu\rho U^2$ is the Alfvén number, and μ is the permeability of the fluid. The electric current and the vorticity have only azimuthal components, being

$$j_\theta = \frac{Br}{\mu}\sqrt{(U/\kappa)}\, g''(\phi),\quad \omega_\theta = Ur\sqrt{(U/\kappa)}\, f''(\phi) \tag{2.9}$$

respectively; the electric field vanishes everywhere. As in the ordinary hydrodynamical problem (the equations for which are found by taking $B = S = 0$ and $\kappa = \nu$ in the above), the equations determining the pressure can be integrated at once; in particular

$$p_1 = Sg'^2 + 1 - S\alpha, \tag{2.10}$$

where we have written the constant of integration as $(1 - S\alpha)$. Substituting this result, (2.5) becomes

$$\frac{\nu}{\kappa} f''' + 2ff'' - f'^2 + 1 = S(2gg'' - g'^2 + \alpha). \tag{2.11}$$

We are at liberty to choose κ in any way we please, but as we are interested only in approximate solutions of the equations for very large and very small values of the diffusion number, it is convenient to take $\kappa = \nu$ when considering layers in which viscosity dominates (i.e., viscous boundary layers), and (usually) $\kappa = \eta$ when considering layers in which diffusion of the lines of force is important (i.e., current layers). For the viscous layers we use F, G and ξ in place of f, g and ϕ, and the equations to be solved are therefore

$$F''' + 2FF'' - F'^2 + 1 = S(2GG'' - G'^2 + \alpha), \tag{2.12}$$

$$G'' = 2\varepsilon(F'G - FG'); \tag{2.13}$$

similarly, in the current layers where we use $\mathscr{F}$, $\mathscr{G}$, and ϑ in place of f, g, and ϕ, the equations become

$$\varepsilon\mathscr{F}''' + 2\mathscr{F}\mathscr{F}'' - \mathscr{F}'^2 + 1 = S(2\mathscr{G}\mathscr{G}'' - \mathscr{G}'^2 + \alpha), \tag{2.14}$$

$$\mathscr{G}'' = 2\mathscr{F}'\mathscr{G} - 2\mathscr{F}\mathscr{G}'. \tag{2.15}$$

Note that $\mathrm{d}G/\mathrm{d}\xi = \mathrm{d}\mathscr{G}/\mathrm{d}\vartheta$ and $G(\xi) = \varepsilon^{-\frac{1}{2}}\mathscr{G}(\vartheta)$, with similar relationships for $F(\xi)$ and $\mathscr{F}(\vartheta)$. For numerical integration of the full equations, it may be convenient to choose $\kappa = \sqrt{(\nu\eta)}$.

Boundary conditions. For stagnation point flow, the boundary conditions to be satisfied by the velocity components are $u = v = 0$ on $z = 0$. and $u \to Ur$ as $z \to \infty$; thus

$$f(0) = f'(0) = 0, \text{ and } f'(\phi) \to 1 \text{ as } \phi \to \infty, \tag{2.16}$$

and we see from (2.6) and (2.9) that the electric current vanishes on the boundary .The tangential components of the magnetic induction must be continuous at the surface $z = 0$. Hence, if dashes are used to denote quantities in the solid region $z \leqslant 0$, then on $z = 0$

$$B'_r/\mu' = Brg'(0)/\mu, \ B'_z = -2B\sqrt{(\kappa/U)}\, g(0), \tag{2.17}$$

and the electric field is zero. We shall consider the case in which no currents flow in the solid region, so that the magnetic field is curl-free; a general solution which enables the boundary conditions to be satisfied is

$$A' = (az + b)\, r^2, \tag{2.18}$$

where $a = Bg'(0)\mu'/\mu$ and $b = B\sqrt{(\kappa/U)}\, g(0)$. The only solution for which there is no field in the solid and the conductivities are finite is the trivial case of zero field everywhere. There are two possible ways in which the conditions on $g(\phi)$ can be chosen; these are:

Case A $\quad g'(\phi) \to 1$ as $\phi \to \infty$, $g(0) = D\sqrt{(U/\kappa)}$, (2.19)

Case B $\quad g(\phi) \to 0$ as $\phi \to \infty$, $g(0) = D\sqrt{(U/\kappa)}$, (2.20)

where D is a constant depending on the form of the magnetic field as $z \to -\infty$. These conditions determine the value of α, for by substituting the values at infinity in (2.11) we find that $\alpha = 1$ in case A, and $\alpha = 0$ in case B.

The stagnation point solution gives a locally valid representation of a large number of possible flows. The solution in case A could represent, for example, the flow near the stagnation point of a sphere which is moving at constant speed along the lines of force of a uniform ambient magnetic field. Similarly the solution in case B could represent the flow near the stagnation point when a magnetised sphere moves at constant speed in the direction of its magnetisation, the magnetic field vanishing at large distances from the sphere. In either case the sphere may contain, say, a suitably aligned dipole at its centre, and (2.18) remains a locally valid solution for the field near the stagnation point. The only condition that must be satisfied is that the boundary is effectively plane at the stagnation point; this is true provided both $\sqrt{(\eta/U)}$ and $\sqrt{(\nu/U)}$ are small compared with the radius of curvature of the body at the stagnation point.

Approximate solutions valid for small diffusion

numbers. For very small values of the diffusion number, viscous effects are negligible in the current layer, so that the appropriate equations for this layer are (2.14) and (2.15) with the term $\varepsilon\mathscr{F}'''$ omitted from (2.14), thus

$$2\mathscr{F}\mathscr{F}'' - \mathscr{F}'^2 + 1 = S(2\mathscr{G}\mathscr{G}'' - G'^2 + \alpha), \tag{2.21}$$

and

$$\mathscr{G}'' = 2\mathscr{F}'\mathscr{G} - 2\mathscr{F}\mathscr{G}'. \tag{2.22}$$

A relatively thin viscous boundary layer occurs next to the boundary, permitting the no-slip condition to be satisfied; this condition is ignored when the above equations for the current layer are solved.

It is not easy to obtain a solution of (2.21) and (2.22) in any given case owing to their behaviour at $\mathscr{F}(\vartheta) = 0$; however, approximate solutions can be sought in series form:

$$\mathscr{G}(\vartheta) = \sum_0^\infty S^n\mathscr{G}_n(\vartheta), \qquad \mathscr{F}(\vartheta) = \sum_0^\infty S^n\mathscr{F}_n(\vartheta).$$

Clearly $\mathscr{F}_0(\vartheta) = \vartheta$ in all cases, and $\mathscr{G}_0(\vartheta)$ satisfies the equation

$$\mathscr{G}_0'' + 2\vartheta\mathscr{G}'_0 - 2\mathscr{G}_0 = 0, \tag{2.23}$$

which has the solution

$$\mathscr{G}_0(\vartheta) = \alpha\vartheta + \mathscr{G}(0)\left(1 - 2\int_0^\vartheta\int_y^\infty \mathrm{e}^{-x^2}\,\mathrm{d}x\,\mathrm{d}y\right). \tag{2.24}$$

Since $\mathscr{G}'_0(0) = \alpha - \pi^{\frac{1}{2}}\mathscr{G}(0)$, the solution in the solid region to this order of approximation is given by

$$A' = \frac{\mu' B r^2}{\mu}\left[\left(\alpha - D\sqrt{\frac{\pi U}{\mu}}\right)z + \mu D/\mu'\right] + O(S). \tag{2.25}$$

The reader will note that the field in the solid region can be uniform (as assumed by Neuringer and McIlroy) only in case A when $D = \sqrt{(\eta/\pi U)}$ if $S = 0$. Solutions for the higher order terms are best obtained numerically if required, but it is interesting to examine the equation for $\mathscr{F}_1(\vartheta)$ which becomes on differentiating

$$\mathscr{F}'''_1 = -2\mathscr{G}_0\mathscr{G}_0''; \tag{2.26}$$

this can be integrated to give

$$\mathscr{F}''_1(\vartheta) = M\int_\vartheta^\infty \mathscr{G}_0(x)\,\mathrm{e}^{-x^2}\,\mathrm{d}x, \tag{2.27}$$

where M is a constant. We see that $\mathscr{F}''_1(0)$ is finite here, although the vorticity is often logarithmically infinite in the $O(S)$ solution for this type of problem (see for example, Ludford and Murray[15]). The solution for $\mathscr{G}_0(\vartheta)$ with $\alpha = 1$ and $D = 0$ has been given previously by Meyer[8]) and Poots and Sowerby[19]); (2.24) and (2.25) represent the general solution for arbitrary D and $\alpha = 0$ or 1.

Compared with the current layer, the viscous boundary layer is so thin when $\varepsilon \ll 1$, that as a first approximation the components of the magnetic field can be taken to be constant; however a certain amount of care is required in order to obtain the correct approximation for the Lorentz force terms in (2.12). From (2.15) we note that in the viscous boundary layer

$$\frac{\mathrm{d}^2 G}{\mathrm{d}\xi^2} = \varepsilon^{\frac{1}{2}} \frac{\mathrm{d}^2 \mathscr{G}}{\mathrm{d}\vartheta^2} \approx 2\varepsilon^{\frac{1}{2}} \mathscr{G}(0) \frac{\mathrm{d}F}{\mathrm{d}\xi} - 2\varepsilon \mathscr{G}'(0)\, F, \tag{2.28}$$

and so

$$\frac{\mathrm{d}}{\mathrm{d}\xi}\left(\frac{\mathrm{d}\mathscr{G}}{\mathrm{d}\vartheta}\right) \approx 2\varepsilon^{\frac{1}{2}} \mathscr{G}(0) \frac{\mathrm{d}F}{\mathrm{d}\xi}. \tag{2.29}$$

Thus the change in $\mathrm{d}\mathscr{G}/\mathrm{d}\vartheta$ across the layer is $O(\varepsilon^{\frac{1}{2}})$, confirming our assertion that the magnetic field is effectively constant in the viscous boundary layer. Hence we see that, correct to $O(\varepsilon^{\frac{1}{2}})$,

$$2GG'' - G'^2 \approx 4\mathscr{G}(0)^2 F' - \mathscr{G}'(0)^2, \tag{2.30}$$

and so an approximate equation for the viscous boundary layer, valid when $\varepsilon \ll 1$, is

$$F''' + 2FF'' - F'^2 + 1 = S(4\mathscr{G}(0)^2 F' - \mathscr{G}'(0)^2 + \alpha). \tag{2.31}$$

The boundary conditions are $F(0) = F'(0) = 0$ and $F'(\xi) \to E$ as $\xi \to \infty$, where E is the positive root of the quadratic equation

$$E^2 + 4S\mathscr{G}(0)^2 E + S(\alpha - \mathscr{G}'(0)^2) - 1 = 0. \tag{2.32}$$

The equation used by Rossow[4]) is a special case of (2.31) with $\mathscr{G}'(0) = 0$ and $\alpha = 1$ (that is, case A), although it is by no means clear from Rossow's presentation that this is the problem being considered. Hess[3]) suggested that the magnetic field in this case would have to arise from a magnet placed in the stream ahead of the stagnation point; this is not a correct interpretation of case A, but it does emphasize that this case is not particularly relevant to aeronautical problems such as re-entry. Clearly there is a need for careful approximations in these problems, since it is doubtful whether the reasoning employed by Rossow [5]) would lead to (2.31) for general values of $\mathscr{G}(0)$ and $\mathscr{G}'(0)$ with $\alpha = 0$ or 1.

In order to solve (2.31), it is first necessary to solve (2.21) and (2.22), so that a value can be obtained for $\mathscr{G}'(0)$. Normally one solves equations of this type numerically by integrating towards the origin ($\mathscr{F} = 0$), starting with suitable asymptotic solutions valid for large values of ϑ. In this case, the procedure is complicated by the term $\mathscr{F}\mathscr{F}''$ in (2.21), which contains the highest derivative of $\mathscr{F}$, but which vanishes at $\vartheta = 0$. A second series solution, valid for small values of ϑ, must therefore be used in place of the numerical solutions when ϑ is small. (Meyer [7]) has obtained some numerical solutions for case B, but does not make this point explicitly). This procedure is not always possible in boundary layer problems of the type $U = cx^m$, as the equations for the current layer have a non-integrable singularity at the boundary when $m \leq 0$ (Lewellen [20])). With $\mathscr{G}'(0)$ known, the solution of (2.31) is straightforward, although one must make use of an asymptotic solution valid for large ξ to start the integration.

This approximate method of solving the stagnation point problem for small values of ε is considerably easier than attempting to solve the full equations (2.6) and (2.11) as they stand. The difficulties encountered in this problem are largely caused by the two-point boundary conditions. If, for example, one tries to solve the full equations by integrating towards the origin, using asymptotic solutions to start, the correct solution must be chosen from a two-parameter family of solutions since the conditions at the boundary leave two arbitrary constants in the asymptotic solutions. The approximate method avoids the difficulty of having to estimate these two parameters concurrently by treating the problem in two steps (that is, as two boundary layers) with one parameter to be determined in each.

For very large values of S, an approximate solution of (2.31) can be found by neglecting the terms other than F''' on the left hand side. The resulting equation is linear and its solution is easily found to be

$$F'(\xi) = \frac{\mathscr{G}'(0)^2 - \alpha}{4\mathscr{G}(0)^2}\,[1 - \exp(-2S^{\frac{1}{2}}\mathscr{G}(0)\,\xi)]. \tag{2.33}$$

It can be shown that this is a Hartmann type of solution 21), with the boundary layer thickness inversely proportional to $S^{\frac{1}{2}}$. Note that the solution indicates that reversed flow can occur in case A if $S \gg 1$; this effect is referred to again at the end of the section. In case B it is likely that no solution exists when $S \gg 1$, since the appropriate solution of (2.21) with the left hand side neglected, cannot be made to satisfy (2.20).

Approximate solutions valid for large diffusion numbers. When the diffusion number is very large, we assume that the flow in the viscous boundary layer is, to a first approximation, that of a perfectly conducting fluid, and the adjustment of the magnetic field to satisfy the boundary conditions at $z = 0$ takes place in a narrow current layer next to the surface. The current layer is not thinner than the viscous boundary layer by a factor $\varepsilon^{-\frac{1}{2}}$ as might be expected to begin with, but a certain negative power of ε is involved, and our assumption that the current layer is negligibly thin for sufficiently large ε can be justified *a posteriori*.

For the viscous boundary layer we neglect the term G''/ε in (2.13), which can then be integrated at once to give

$$G = \alpha F. \tag{2.34}$$

This result can be substituted into (2.12) to give a single equation for $F(\xi)$; in case B this is simply the ordinary Homann equation, and in case A the equation is

$$F''' + (1 - S)(2FF'' - F'^2 + 1) = 0. \tag{2.35}$$

If $S < 1$, we can make the transformation

$$F(\xi) = (1 - S)^{-\frac{1}{2}}\Theta(x), \quad x = (1 - S)^{\frac{1}{2}}\xi, \tag{2.36}$$

so that (2.35) also reduces to the Homan equation

$$\Theta''' + 2\Theta\Theta'' - \Theta'^2 + 1 = 0, \tag{2.37}$$

with boundary conditions $\Theta(0) = \Theta'(0) = 0$, $\Theta'(\infty) = 1$. Note that the transformation shows that the effect of the magnetic field is formally equivalent to an alteration of the kinematic viscosity from ν to $\nu/(1 - S)$ *) if $S < 1$; the viscous boundary layer thickness is correspondingly greater by a factor $(1 - S)^{-\frac{1}{2}}$.

---

*) F. A. Goldsworthy (private communication).

When the Alfvén number exceeds unity, there is no solution of (2.35) if the flow is directed towards the boundary *), but there is a solution if the flow is reversed. That is, taking U to be positive as before if $u \rightarrow -Ur$ as $z \rightarrow \infty$, (2.16) is amended to $f'(\phi) \rightarrow -1$ as $\phi \rightarrow \infty$. We regain the Homann equation (2.37) once again by making the transformation

$$F(\xi) = -(S-1)^{-\frac{1}{2}}\Theta(y),\ y = (S-1)^{\frac{1}{2}}\xi, \tag{2.38}$$

in (2.35); the boundary conditions, as before, are $\Theta(0) = \Theta'(0) = 0$, $\Theta'(\infty) = 1$. In this case the effect of the magnetic field is equivalent to altering the kinematic viscosity to $\nu/(S-1)$, thus changing the thickness of the viscous boundary layer by a factor $(S-1)^{-\frac{1}{2}}$. There appears to be no solution of the stagnation point problem when $S = 1$.

It is assumed that the current layer is so much thinner than the viscous boundary layer that the velocity profile in the current layer is effectively linear; thus (2.15) can be written

$$\mathscr{G}'' + 2\beta\vartheta^2\mathscr{G}' - 4\beta\vartheta\mathscr{G} = 0, \tag{2.39}$$

if $\mathscr{F}(\vartheta) \approx \beta\vartheta^2$ in this region. In case B, it is found that $\beta = 0.656\varepsilon^{-\frac{1}{2}}$, and in case A

$$\beta = 0.656(1-S)^{\frac{1}{2}}/\varepsilon^{\frac{1}{2}},\ (S<1);\ \beta = -0.656(S-1)^{\frac{1}{2}}/\varepsilon^{\frac{1}{2}},\ (S>1). \tag{2.40}$$

To obtain the correct scale for the current layer we must make a change of independent variable to

$$\lambda = \beta^{\frac{1}{3}}\vartheta, \tag{2.41}$$

so that (2.39) becomes

$$\frac{\mathrm{d}^2\mathscr{G}}{\mathrm{d}\lambda^2} + 2\lambda^2\frac{\mathrm{d}\mathscr{G}}{\mathrm{d}\lambda} - 4\lambda\mathscr{G} = 0. \tag{2.42}$$

Thus the scale of the current layer is not $\sqrt{(\eta/U)}$ as it is when $\varepsilon \ll 1$, but instead it is $\beta^{-\frac{1}{3}}\sqrt{(\eta/U)}$. The ratio of the thickness of the current layer to that of the viscous boundary layer is $O(\varepsilon^{-\frac{1}{3}})$, which justifies our original assumption that this ratio is small for large diffusion numbers. Correspondingly, the ratio of the term neglected in (2.13) to those retained is $G''/\varepsilon GF' \approx O(1/\varepsilon\xi^3)$ near $\xi = 0$, which is not small when $\xi = O(\varepsilon^{-\frac{1}{3}})$ and indicates the necessity for a current sheet at the boundary. By substituting $\kappa = \eta/\beta^{\frac{2}{3}}$ in (2.11) we see that $\mathrm{d}^3\mathscr{F}/\mathrm{d}\lambda^3 = O(\varepsilon^{-1}\lambda^2)$, and hence the solution $\mathscr{F}(\vartheta) = \beta\vartheta^2$ is valid in the current layer provided $\lambda \ll \varepsilon^{\frac{1}{3}}$.

---

*) Since the Homann equation cannot be solved with the boundary condition $\Theta'(\infty) = -1$.

Note that (2.42) has the asymptotic solution

$$\mathscr{G}(\lambda) \sim N_1 \int_{\lambda}^{\infty} \mathrm{e}^{-2\lambda^3/3}\, \mathrm{d}\lambda + N_2[\lambda^2 + O(\lambda^{-1})], \tag{2.43}$$

for large λ, where N_1 and N_2 are constants. Clearly $N_2 = 0$ in case B since $\mathscr{G}(\lambda) \to 0$ as $\lambda \to \infty$; in case A, $\mathscr{G} \sim \mathscr{F}$ as $\lambda \to \infty$, so that $N_2 = \beta^{\frac{1}{3}}$.

The behaviour of the solution for case A is particularly interesting. It is a feature of magnetohydrodynamics that vorticity is not only diffused by viscosity but is also propagated along the lines of force as magnetohydrodynamic waves. In this example the vorticity produced as a result of the no-slip condition is diffused by viscosity to form a boundary layer and at the same time tends to be propagated away from the surface. When $S < 1$, the speed of propagation of magnetohydrodynamic waves is less than the fluid speed, and so the vorticity remains confined to the neighbourhood of the boundary, although the tendency to propagate is made evident by the increase in the boundary layer thickness. When $S > 1$, the vorticity can move freely against the stream and so does not remain in the form of a boundary layer when the flow is directed towards the boundary: in other words the boundary layer does not exist because there is no longer any balance between convection and diffusion of vorticity. If the stream direction is reversed, however, the vorticity which moves against the stream remains next to the boundary, and the boundary layer is kept intact; in this case the solution refers to a reversed stagnation point, and the flow away from the boundary represents a wake.

The vorticity argument given here does not apply when the diffusion number is very small, and so it is not immediately clear whether or not the reversed stagnation point flow is possible in this case. Solutions of (2.21) and (2.22) appear to be possible when the condition at infinity is amended to $\mathscr{F}'(\infty) = -1$ and both roots of (2.32) are negative in case A if $S > 1/[1 - \mathscr{G}'/0)^2] \geq 1$, so that a solution of the viscous boundary layer equation (2.31) should also be possible for reversed flow. A final answer to this question must be left until an attempt is made to solve the equations numerically.

§ 3. *Stagnation point flow with a purely azimuthal magnetic field.* When the magnetic field is produced by an axial current and is therefore of the form $(0, B_\theta, 0)$, a solution of the stagnation point flow problem can be found with the stream function ψ defined as in (2.1) and with the magnetic induction given by

$$B_\theta = \bar{B} r h(\phi), \tag{3.1}$$

where $\bar{B}$ is a constant with dimensions (magnetic induction/length). The total magnetic and fluid pressure χ has the form

$$\chi = p + B_\theta{}^2/8\pi\mu = \chi_0 - \tfrac{1}{2}\rho U^2 r^2 \chi_1(\phi) - 2\rho U \kappa \chi_2(\phi), \tag{3.2}$$

where χ_0 is a constant. The functions $f(\phi)$, $h(\phi)$, $\chi_1(\phi)$ and $\chi_z(\phi)$ are found to satisfy the following set of ordinary differential equations:

$$\frac{\nu}{\kappa} f''' + 2ff'' - f'^2 + \chi_1 = Sh^2, \tag{3.3}$$

$$\chi'_1 = 0, \tag{3.4}$$

$$\chi'_2 = \left(\frac{\nu}{\kappa} f' + f^2\right)', \tag{3.5}$$

$$\frac{\eta}{\kappa} h'' + 2fh' = 0, \tag{3.6}$$

where $S = \bar{B}^2/4\pi\mu\rho U^2$.

The boundary conditions are taken to be

$$f(0) = f'(0) = 0, \; f'(\phi) \to 1 \text{ as } \phi \to \infty, \tag{3.7}$$

$$h(0) = \tau, \; h(\phi) \to \gamma \text{ as } \phi \to \infty, \tag{3.8}$$

where γ and τ are constants. Equation (3.4) shows that χ_1 is a constant, and we see from (3.3) that this must be

$$\chi_1 = 1 + S\gamma^2; \tag{3.9}$$

thus (3.3) becomes

$$\frac{\nu}{\kappa} f''' + 2ff'' - f'^2 + 1 = S(h^2 - \gamma^2). \tag{3.10}$$

A suitable solution for the solid region is

$$B'_\theta = \bar{B}' r(1 + D'z), \tag{3.11}$$

representing an axial current; in order to satisfy the condition that the tangential component of the magnetic field should be continuous, $\tau = \bar{B}'\mu/\bar{B}\mu'$. Note that if $\gamma = \tau$, then $h(\phi)$ is constant everywhere and (3.10) reduces to the Homann equation on putting $\kappa = \nu$. The magnetic field has no effect on the motion in this case, whatever the value of S, since on convection a tube of force replaces and is replaced by an exactly equivalent tube of force. Convective interchange of tubes of force in this manner is important in certain geophysical problems 17), and it has also been discussed by Michael 18) in relation to a stability problem.

As in the previous section, we use F, H, ξ to denote f, h, ϕ when κ is chosen to be ν, and $\mathscr{F}$, $\mathscr{G}$, ϑ when κ is chosen to be η.

Approximate solutions valid for large diffusion numbers. For large values of the diffusion number the fluid may be considered to be perfectly conducting everywhere outside a thin current layer situated next to the boundary. The solution for the flow outside this current layer is found by putting $\kappa = \nu$ and neglecting the term H''/ε in (3.6) which becomes

$$H'(\xi) = 0. \tag{3.12}$$

Hence the magnetic field is given by $H(\xi) = \text{constant} = \gamma$, and (3.10) reduces to the Homann equation for $F(\xi)$.

In the current layer, it is sufficiently accurate to take $\mathscr{F}(\vartheta) \approx \beta\vartheta^2$ where $\beta = 0.656/\varepsilon^{\frac{1}{2}}$; equation (3.6) therefore reduces to

$$\mathscr{H}'' + 2\beta\vartheta^2\mathscr{H}' = 0, \tag{3.13}$$

which has the solution

$$\mathscr{H}(\vartheta) = \tau + (\gamma - \tau)\,(\int_0^{\vartheta} \mathrm{e}^{-2\beta x^3/3}\,\mathrm{d}x)/(\int_0^{\infty} \mathrm{e}^{-2\beta x^3/3}\,\mathrm{d}x). \tag{3.14}$$

As was found in the previous section, the ratio of the thickness of the current layer to that of the viscous boundary layer is $0(\varepsilon^{-\frac{1}{3}})$ when $\varepsilon \gg 1$.

Approximate solutions valid for small diffusion numbers. Proceeding as before, we consider first the current layer which envelopes the viscous boundary layer when $\varepsilon \ll 1$. Taking $\kappa = \eta$ and neglecting the term $\varepsilon\mathscr{F}'''$ in (3.10), we obtain the following equations for the current layer:

$$2\mathscr{F}\mathscr{F}'' - \mathscr{F}'^2 + 1 = S(\mathscr{H}^2 - \gamma^2), \tag{3.15}$$

$$\mathscr{H}'' + 2\mathscr{F}\mathscr{H}' = 0. \tag{3.16}$$

In this case the solution in ascending powers of S yields $\mathscr{F}_0(\vartheta) = \vartheta$ and $\mathscr{H}_0(\vartheta) = \tau + (\gamma - \tau)\ \mathrm{erf}\ \vartheta$. Numerical integration of these equations for finite values of S can be carried out by the method described in the last section, but this is not necessary if one is interested only in the viscous boundary layer.

For the solution in the viscous boundary layer, we put $\kappa = \nu$ and neglect the term $\varepsilon FH'$ in equation (3.6). Thus $H''(\xi) = 0$ and so $H(\xi) = \tau$ to a good approximation in this region. Substituting this result in (3.10) we obtain

$$F''' + 2FF'' - F'^2 + 1 = S(\tau^2 - \gamma^2), \tag{3.17}$$

which reduces to the Homann equation (2.37) on making the transformation

$$F(\xi) = L\Theta(\lambda),\ \lambda = L\xi, \tag{3.18}$$

where

$$L^4 = 1 + S(\gamma^2 - \tau^2). \tag{3.19}$$

From (3.17) we see that $F'(\xi) \to L^2$ as $\xi \to \infty$, and so the boundary conditions on $\Theta(\lambda)$ remain $\Theta(0) = \Theta'(0) = 0$, $\Theta'(\infty) = 1$. It appears that in cases where $\tau > \gamma$ a sufficiently large value of S causes the solution to break down, since L^4 becomes negative. In particular, if $\gamma = 0$ and $\tau = 1$, the breakdown occurs when $S \geq 1$, indicating that the kinetic energy density of the flow is less than the field energy density, and so the fluid cannot convect the current away from the stagnation point. It should be noted that there is no possibility of reversed flow in this instance as $F'(\infty) = L^2$ becomes imaginary at the point of breakdown, and this cannot be altered by a simple change of sign in the velocity.

This result may be of interest to experiments since it shows that very strong magnetohydrodynamic boundary layer effects can be demonstrated despite the small values of ε obtainable in the laboratory. The author doubts that a flow could be made to 'choke up' in practice as an instability would probably occur causing axial symmetry to be lost; nevertheless, the trend towards choking could be demonstrated for values of S slightly less than unity.

Received 6th February, 1961.

REFERENCES

1) Michael, D. H., Mathematika **1** (1954) 131.
2) Neuringer, J. L. and W. McIlroy, J. Aero Sci. **25** (1958) 194.
3) Hess, R. V., A. R. C. Report No. 21, 113, 1959.
4) Rossow, V. J., J. Aero. Sci. **25** (1958) 334.
5) Rossow, V. J., Nat. Adv. Comm. Aero. Wash., Tech. Note, No. 3971, 1957.
6) Axford, W. I., J. Fluid Mech. **8** (1960) 97.
7) Meyer, R. X., Z. angew. Math. Phys. **11** (1960) 127.
8) Meyer, R. C., J. Aero. Sci. **25** (1958) 561.
9) Kakutani, T., J. Phys. Soc. Japan **15** (1960) 688.
10) Oguchi, H., Phys. Fluids **3** (1960) 567.
11) Batchelor, G. K., Proc. Roy. Soc. A **210** (1950) 405.
12) Greenspan, H. P. and G. F. Carrier, J. Fluid Mech. **6** (1959) 77.
13) Homann, F., See for example: H. Schlichting, Boundary Layer Theory, Pergamon Press, London, 1955, Page 73.
14) Goldstein, S., Modern Developments in Fluid Mechanics, Vol. II, Oxford 1938, Chapter XIV.
15) Ludford, G. S. and J. P. Murray, J. Fluid Mech. **7** (1960) 516.
16) Yih, C. S., Phys. Fluids **2** (1959) 125.
17) Gold, T., J. Geophys. Res. (1959) 1219.
18) Michael, D. H., Mathematika **1** (1954) 45.
19) Poots, G. and L. Sowerby, Quart. J. Mech. Appl. Math. **13** (1960) 385.
20) Lewellen, W. S., Cornell Graduate School of Engineering Report AFOSR–TN–59–927, 1960.
21) Hartman, J., Math.-fys. Medd. **15** (1937) No. 6.

Appl. sci. Res.   Section B, Vol. **9**

THE FLOW OF A CONDUCTING FLUID PAST A MAGNETIZED CYLINDER AT HIGH MAGNETIC REYNOLDS NUMBERS

by L. M. HOCKING

University College, London, England

Summary

A conducting, inviscid fluid flowing past a magnetized cylinder changes the magnetic field outside and inside the cylinder. This field is found for a cylinder magnetized as a dipole, with the restrictions that (a) the magnetic field is weak and (b) the magnetic Reynolds number is large. The magnetic field in turn alters the velocity field by the generation of vorticity, and the new velocity field and the resulting drag are found when the direction of the dipole is parallel to the free stream.

§ 1. *Introduction and formulation.* The flow of an inviscid, incompressible, conducting fluid past a magnetized cylinder is considered in this paper for cases where the ratio of the magnetic to the dynamic pressure is small, but the magnetic Reynolds number is large. This implies that the magnetic field is considerably distorted from its value when the fluid is non-conducting, but the velocity field is only slightly altered. The magnetic Reynolds number is defined by $R_M = LU\mu\sigma$, where L and U are a typical length and velocity respectively and μ is the permeability and σ the conductivity of the fluid, so that large values of R_M can occur, for example, in astrophysical problems, when the large values of L will outweigh the small values of σ. The natural problem to consider for astrophysical application would be the flow past a sphere, but this is a considerably more difficult problem than the flow past a cylinder, and the methods used here cannot be adapted to the spherical problem, even when the magnetic field is aligned to maintain axial symmetry.

When R_M is large, the magnetic field tends to be aligned with the velocity, so that a magnetic line emerging from the cylinder is swept round the cylinder by the fluid, and the magnetic field is confined to a boundary layer and a narrow wake stretching downstream from the rear stagnation point. This magnetic field exerts a non-conservative body-force on the fluid, producing vorticity and hence modifying the velocity field. It should be made clear that the basic velocity field is the simple potential flow with no separation of the flow from the cylinder. Obviously, a model which included separation would be more realistic but also much more complicated.

Similar problems to that considered in this paper, but for small values of R_M, have been solved by Ludford and Murray [1]) and Murray and Chi [2]) for a sphere and a cylinder, respectively. In the present paper, a method is devised for finding the magnetic field for cylinders of arbitrary cross-section and for any value of R_M, and the particular case of large R_M and a circular cylinder magnetized as a dipole is considered. When the dipole is aligned with the free stream, the new velocity field and the drag are found.

The equations satisfied by the velocity and magnetic fields are, in non-dimensional form,

$$\begin{aligned} \operatorname{curl}\boldsymbol{q} \times \boldsymbol{q} &= -\nabla(p + \tfrac{1}{2}q^2) + \beta \operatorname{curl} \boldsymbol{H} \times \boldsymbol{H}, \\ \operatorname{curl} \boldsymbol{H} &= R_M \boldsymbol{q} \times \boldsymbol{H}, \\ \operatorname{div} \boldsymbol{H} &= \operatorname{div} \boldsymbol{q} = 0, \end{aligned}$$

where $\beta = \mu h^2/\rho U^2$, L, U and h are the units of length, velocity and magnetic field, and ρ is the density of the fluid. As in Murray and Chi [2]) the electric field has been made zero, which is consistent if no current flows at infinity. The parameter β is the ratio of the magnetic and dynamic pressure and is supposed to be small so that an expansion in powers of β can be made. With $\boldsymbol{q} = \boldsymbol{q}_0 + \beta\boldsymbol{q}_1 + \ldots$, $p = p_0 + \beta p_1 + \ldots$ and $\boldsymbol{H} = \boldsymbol{H}_0 + \beta\boldsymbol{H}_1 + \ldots$, where $\boldsymbol{q}_0$ and p_0 are the velocity and pressure in the absence of any magnetic field, the equations for $\boldsymbol{H}_0$ and $\boldsymbol{q}_1$ are

$$\operatorname{curl} \boldsymbol{H}_0 = R_M \boldsymbol{q}_0 \times \boldsymbol{H}_0, \tag{1}$$

$$\operatorname{div} \boldsymbol{H}_0 = 0, \tag{2}$$

$$\operatorname{curl} \boldsymbol{q}_1 \times \boldsymbol{q}_0 = -\nabla P_1 + \beta \operatorname{curl} \boldsymbol{H}_0 \times \boldsymbol{H}_0, \tag{3}$$

$$\operatorname{div} \boldsymbol{q}_1 = 0, \tag{4}$$

where $P_1 = p_1 + \boldsymbol{q}_0 \cdot \boldsymbol{q}_1$.

It is convenient to introduce a potential A defined by

$$H_r = \frac{\partial A}{r\,\partial\theta}, \quad H_\theta = -\frac{\partial A}{\partial r},$$

where r and θ are polar coordinates. It was pointed out by Michael[3]) that the equation (1) in terms of A, which he derived for a similar problem with an externally applied magnetic field, is identical with that for temperature in the convection of heat from a cylinder by an inviscid stream of fluid. It is well-known that this equation can be put in a simple form by using the velocity potential and stream function of the irrotational flow as coordinates. For a circular cylinder, if

$$\varphi = \cos\theta\,(r^2+1)/2r, \quad \psi = \sin\theta\,(r^2-1)/2r,$$

so that 2φ and 2ψ are the velocity potential and stream function, the equation becomes

$$\frac{\partial^2 A}{\partial\varphi^2} + \frac{\partial^2 A}{\partial\psi^2} = 2R_M \frac{\partial A}{\partial\varphi}, \tag{5}$$

and the boundary of the cylinder in the (φ, ψ)-plane is $|\varphi| < 1$, $\psi = 0$. A similar transformation will yield the same equation and the same boundary for *any* cylinder.

A method of solving this equation in the heat convection problem was devised by Piercy and Winny[4]) and is used in this paper. The method consists of taking a distribution of fundamental singular solutions of (5) on the cylinder and using the boundary conditions to determine the density of the distribution. The fundamental solutions required are

$$\exp(R_M\varphi)\,K_0[R_M(\varphi^2+\psi^2)^{\frac{1}{2}}], \quad \frac{\partial}{\partial\psi}\{\exp(R_M\varphi)\,K_0[R_M(\varphi^2+\psi^2)^{\frac{1}{2}}]\},$$

which will be called a 'pole' and a 'dipole' respectively, since they reduce to those forms when $R_M = 0$. The direction of the 'dipole' is parallel to the ψ-axis. If a distribution of 'poles' only is taken, the value of the magnetic potential at any point is

$$A = \int_{-1}^{1} u(\xi)\exp[R_M(\varphi-\xi)]\,K_0\{R_M[(\varphi-\xi)^2+\psi^2]^{\frac{1}{2}}\}\,d\xi, \tag{6}$$

where $u(\xi)$ is the density of the distribution at the point $\varphi = \xi$,

$\psi = 0$ on the cylinder. Similarly, a distribution of 'dipoles' only gives

$$A = \int_{-1}^{1} v(\xi) \exp[R_M(\varphi - \xi)] \; \frac{\partial}{\partial \psi} K_0\{R_M[(\varphi - \xi)^2 + \psi^2]^{\frac{1}{2}}\} \, d\xi, \quad (7)$$

with $v(\xi)$ as the density of the distribution.

The 'pole' distribution (6) makes A an even function of ψ. The value of $\partial A/\partial \psi$ on $\psi = 0$ is 0 if $|\varphi| > 1$, but if $|\varphi| < 1$,

$$\left.\frac{\partial A}{\partial \psi}\right|_{\psi=0} = \lim_{\psi \to 0} \int_{-1}^{1} u(\xi) \exp[R_M(\varphi - \xi)] \, \frac{\psi}{[\varphi - \xi)^2 + \psi^2]^{\frac{1}{2}}} \cdot$$
$$\cdot \; K'_0\{R_M[(\varphi - \xi)^2 + \psi^2]^{\frac{1}{2}}\} \, d\xi.$$

Expanding the integrand, the only singular part comes from the neighbourhood of the point $\xi = \varphi$, so that

$$\left.\frac{\partial A}{\partial \psi}\right|_{\psi=0} = \lim_{\psi \to 0} - \psi u(\varphi) \int_{-1}^{1} \frac{d\xi}{(\varphi - \xi)^2 + \psi^2} = \begin{cases} -\pi u(\varphi) & \text{if } \psi \to 0+, \\ +\pi u(\varphi) & \text{if } \psi \to 0-. \end{cases} \quad (8)$$

Similarly, for the 'dipole' distribution (7)

$$A|_{\psi=0} = \mp \pi v(\varphi), \quad (9)$$

and

$$\left.\frac{\partial A}{\partial \psi}\right|_{\psi=0} = \int_{-1}^{1} v(\xi) \exp[R_M(\varphi - \xi)] \, \frac{\partial^2}{\partial \psi^2} K_0\{R_M[(\varphi - \xi)^2 + \psi^2]^{\frac{1}{2}}\} \, d\xi,$$

$$= \int_{-1}^{1} v(\xi) \left(2R_M \frac{\partial}{\partial \varphi} - \frac{\partial^2}{\partial \varphi^2}\right) \{\exp[R_M(\varphi - \xi)] K_0[R_M|\varphi - \xi|]\} d\xi, \quad (10)$$

using (5).

As in Murray and Chi's paper the magnetic field is supposed to originate inside the cylinder as a dipole field. If the direction of the dipole is perpendicular to the direction of the free stream, A must be an even function of ψ by symmetry, and the solution can be found by a distribution of 'poles' only. When the dipole is parallel to the free stream, A is odd in ψ, and the 'dipole' distribution (7) must be used. Since (5) is linear in A, a dipole at any angle requires a linear combination of the two special cases, so that only these need be considered.

The conductivity of the cylinder is finite, so that the field inside the cylinder is modified by the motion of the conducting fluid outside. If A' determines the field inside, A' is a harmonic function which contains a singular term, giving the dipole field, as well as terms finite inside the cylinder. The boundary conditions which link A and A' are the continuity of tangential magnetic field and normal magnetic induction. Thus, in the (r, θ) plane, on $r = 1$

$$\frac{\partial A}{\partial r} = \frac{\partial A'}{\partial r}, \quad \mu A = \mu' A', \tag{11}$$

where μ and μ' are the permeabilities of the fluid and the cylinder respectively. Also, on $r = 1$,

$$\frac{\partial A}{\partial r} = \frac{\partial A}{\partial \psi}\frac{\partial \psi}{\partial r} + \frac{\partial A}{\partial \varphi}\frac{\partial \varphi}{\partial r} = \sin\theta \frac{\partial A}{\partial \psi}.$$

§ 2. *Dipole pointing upstream.* When the dipole in the cylinder is pointing upstream, the appropriate form for the field inside is

$$A' = -\frac{\sin\theta}{r} + \sum_{n=1}^{\infty} a_n r^n \sin n\theta, \tag{12}$$

and for the field outside, A is given by (7). The boundary conditions on the upper surface of the cylinder give

$$\int_{-1}^{1} v(\xi)\left(2R_M \frac{\partial}{\partial \varphi} - \frac{\partial^2}{\partial \varphi^2}\right) \exp[R_M(\varphi - \xi)]\, K_0(R_M|\varphi - \xi|)\, d\xi = \\ = \frac{1}{\sin\theta} \frac{\partial A'}{\partial r}\bigg|_{r=1}, \tag{13}$$

$$-\pi v(\varphi) = \frac{\mu'}{\mu} A'|_{r=1}, \tag{14}$$

with $0 < \theta < \pi$ and $\varphi = \cos\theta$. The boundary conditions on the lower surface are also satisfied since A and A' are even functions of ψ. If R_M is small, the solution can be found by expanding in powers of R_M. However, this is the case considered by Murray and Chi, and the solution obtained by the present method agrees with their solution so the details will not be given here. It would not be difficult to find further terms in the R_M expansion, but the main features of the magnetic field for small R_M are determined by the term already found, so that it is more interesting to consider large values of R_M.

The asymptotic value of the Bessel function for large R_M and $|\varphi - \xi|$ not small is

$$K_0(R_M|\varphi - \xi|) = \left(\frac{\pi}{2R_M}\right)^{\frac{1}{2}} (|\varphi - \xi|)^{-\frac{1}{2}} \exp(-R_M|\varphi - \xi|)[1 + O(R_M{}^{-1})].$$

If the contribution from the small neighbourhood of the point $\xi = \varphi$, in which $R_M|\varphi - \xi|$ is not large, is neglected, the integrand in(13) is

$$(2\pi R_M)^{\frac{1}{2}} \frac{\partial}{\partial\varphi} [v(\xi)(\varphi - \xi)^{-\frac{1}{2}}]$$

if $\xi < \varphi$ and is exponentially small if $\xi > \varphi$, so that (13) becomes

$$(2\pi R_M)^{\frac{1}{2}} \frac{\partial}{\partial\phi} \int_{-1}^{\varphi} \frac{v(\xi)}{(\varphi - \xi)^{\frac{1}{2}}} \mathrm{d}\xi = \frac{1}{\sin\theta} \left.\frac{\partial A'}{\partial r}\right|_{r=1}. \tag{15}$$

To solve this equation and (14), write

$$A' = -\frac{\sin\theta}{r} + r\sin\theta + \frac{1}{R_M{}^{\frac{1}{2}}} A'_1 + \ldots,$$

$$v = \frac{1}{R_M{}^{\frac{1}{2}}} v_1 + \ldots,$$

so that the leading terms are given by

$$(2\pi)^{\frac{1}{2}} \frac{\partial}{\partial\varphi} \int_{-1}^{\varphi} \frac{v_1(\xi)}{(\varphi - \xi)^{\frac{1}{2}}} \mathrm{d}\xi = 2, \tag{16}$$

$$A'_1|_{r=1} = -\frac{\pi\mu}{\mu'} v_1(\varphi). \tag{17}$$

The integral equation for v_1 can be written

$$\int_{-1}^{\varphi} \frac{v_1(\xi)}{(\varphi - \xi)^{\frac{1}{2}}} \mathrm{d}\xi = \left(\frac{2}{\pi}\right)^{\frac{1}{2}} (\varphi + k),$$

where k is some constant, and the solution of this equation is

$$v_1(\xi) = \frac{2}{\pi}\left(\frac{2}{\pi}\right)^{\frac{1}{2}} \frac{\partial}{\partial\xi} \int\limits_{-1}^{\xi} \frac{(\varphi + k)\, d\varphi}{(\xi - \varphi)^{\frac{1}{2}}} = \frac{2}{\pi}\left(\frac{2}{\pi}\right)^{\frac{1}{2}} (\xi + 1)^{\frac{1}{2}}, \quad (18)$$

where k has been chosen so that v_1 is finite at $\xi = -1$. The value of A'_1 on the cylinder is given by (17) as

$$A'_1|_{r=1} = -\frac{4\mu}{\pi^{\frac{1}{2}}\mu'} \cos \tfrac{1}{2}\theta,\ 0 < \theta < \pi, \quad (19)$$

and since A' is an odd harmonic function, the value of the potential inside the cylinder is easily found to be

$$A' = -\frac{\sin\theta}{r} + r\sin\theta - \frac{32\mu}{\pi\mu'(\pi R_M)^{\frac{1}{2}}} \sum_{n=1}^{\infty} \frac{n}{4n^2 - 1} r^n \sin n\theta. \quad (20)$$

The value of A so far obtained has a discontinuity at the rear stagnation point, $\varphi = 1$. Mathematically, this has appeared because the contribution of the neighbourhood of the point $\xi = \varphi$ to the integral (13) cannot be neglected when $\varphi = 1$. The magnetic field is shown by (20) to be almost confined to the interior of the cylinder, but there are magnetic lines, for small values of A of order $R_M^{-\frac{1}{2}}$, which leave the cylinder at all points, re-entering the cylinder at the rear stagnation point. If the neglected part of (13) were included, it would show that the re-entry took place over a region near the stagnation point with a width of order R_M^{-1}.

The field outside the cylinder is given by (7) and (18). Using the asymptotic expansion of the Bessel function to the same order as used in satisfying the boundary conditions, $A = 0$ if $\varphi < -1$, *i.e.* upstream from the cylinder and, if $|\varphi| < 1$,

$$A = -\frac{2}{\pi} \int\limits_{-1}^{\varphi} \frac{(1 + \xi)^{\frac{1}{2}}\psi}{[(\varphi - \xi)^2 + \psi^2]^{\frac{3}{4}}} \exp[-R_M\psi^2/2(\varphi - \xi)]\, d\xi. \quad (21)$$

The magnetic field is negligible outside the boundary layer defined by

$$R_M\psi^2 = 2\lambda(\varphi + 1) \quad (22)$$

where λ is some constant such that $\exp\lambda$ is large compared with 1.

In the effective part of the integral in (21), $R_M(\varphi - \xi)$ is large and $\psi/(\varphi - \xi)$ is small. Defining new variables by

$$\zeta^2 = \frac{R_M\psi^2}{2(\varphi - \xi)}, \quad z_1{}^2 = \frac{R_M\psi^2}{2(\varphi + 1)} \tag{23}$$

and neglecting ψ in comparison with $(\varphi - \xi)$ in the denominator,

$$A = -\frac{4}{\pi}\left[\frac{2(\varphi + 1)}{R_M}\right]^{\frac{1}{2}} \int_{z_1}^{\infty} \left(1 - \frac{z_1{}^2}{\zeta^2}\right)^{\frac{1}{2}} \exp(-\zeta^2)\, \mathrm{d}\zeta. \tag{24}$$

After some manipulation, this can be written

$$A = -\frac{2}{\pi}\left[\frac{2\pi(\varphi + 1)}{R_M}\right]^{\frac{1}{2}} \left[\exp(-z_1{}^2) - 2z_1 \int_{z_1}^{\infty} \exp(-\zeta^2)\, \mathrm{d}\zeta\right]. \tag{25}$$

On the cylinder $z_1 = 0$, and (25) gives the same value of A as can be found from (19).

Downstream from the cylinder,

$$A = -\frac{2}{\pi} \int_{-1}^{1} \frac{(1 + \xi)^{\frac{1}{2}}\psi}{[(\varphi - \xi)^2 + \psi^2]^{\frac{3}{4}}} \exp[-R_M\psi^2/2(\varphi - \xi)]\, \mathrm{d}\xi \tag{26}$$

with $\varphi > 1$, so that A is negligible outside a wake defined by the same expression as the boundary layer (22). In the wake, by the same methods as those used above, the value of A is

$$A = -\frac{4}{\pi}\left[\frac{2(\varphi + 1)}{R_M}\right]^{\frac{1}{2}} \int_{z_1}^{z_2} \left(1 - \frac{z_1{}^2}{\zeta^2}\right)^{\frac{1}{2}} \exp(-\zeta^2)\, \mathrm{d}\zeta, \tag{27}$$

where z_1 is defined in (23) and

$$z_2{}^2 = \frac{R_M\psi^2}{2(\varphi - 1)}.$$

At points in the wake sufficiently far from the cylinder for $\varphi - \xi$ to be replaced by its average value φ in (26)

$$A = -\frac{8\sqrt{2}\psi}{3\pi\varphi^{\frac{3}{2}}} \exp(-R_M\psi^2/2\varphi),$$

or, since in this region $\varphi \simeq \frac{1}{2}r \cos \theta = \frac{1}{2}x$ and $\psi \simeq \frac{1}{2}r \sin \theta = \frac{1}{2}y$,

$$A = -\frac{16y}{3\pi x^{\frac{3}{2}}} \exp(-R_M y^2/4x). \tag{28}$$

Traversing the positive side of the wake, keeping x fixed, A decreases from 0 on the axis to a minimum value

$$-\frac{16}{3\pi x}\left(\frac{2}{R_M e}\right)^{\frac{1}{2}} \quad \text{at} \quad y = (2x/R_M)^{\frac{1}{2}}$$

and then tends rapidly to 0. As R_M increases, each magnetic line moves towards the cylinder and narrows until $A = 0$ everywhere outside the cylinder. The limiting value of the magnetic field as R_M tends to infinity is zero except on the cylinder, where there is a tangential component of magnitude $2 \sin \theta$ directed towards the rear stagnation point, and on the downstream axis, where there is a field of magnitude $16/3\pi x^{\frac{3}{2}}$ for large x, directed towards the cylinder.

A sketch of the magnetic lines for large R_M is shown in fig. 1.

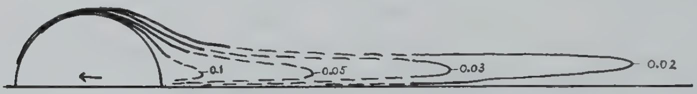

Fig. 1. The magnetic lines when the dipole is aligned with the stream. The full lines are calculated from equations (25) and (28) for $R_M = 100$, and the broken lines are sketched to connect the calculated values.

§ 3. *Dipole perpendicular to the free stream.* When the dipole is at right angles to the direction of the free stream, the appropriate form for the field inside is

$$A' = -\frac{\cos \theta}{r} + \sum_{n=1}^{\infty} a_n r^n \cos n\theta,$$

and the field outside is given by (6). The boundary conditions on the upper surface of the cylinder give

$$-\pi u(\varphi) = \frac{1}{\sin \theta} \frac{\partial A'}{\partial r}\bigg|_{r=1}, \tag{29}$$

$$\int_{-1}^{1} u(\xi) \exp[R_M(\varphi - \xi)]\, K_0(R_M\, |\varphi - \xi|)\, \mathrm{d}\xi = \frac{\mu'}{\mu} A'\big|_{r=1}. \tag{30}$$

As before, the solution for small R_M, found by an expansion in powers of R_M, yields the same results as were found by Murray and Chi. For large values of R_M the asymptotic expansion of the Bessel function replaces (30) by

$$\left(\frac{\pi}{2R_M}\right)^{\frac{1}{2}} \int_{-1}^{\varphi} \frac{u(\xi)}{(\varphi-\xi)^{\frac{1}{2}}}\, \mathrm{d}\xi = \frac{\mu'}{\mu} A'\big|_{r=1}. \tag{31}$$

Writing

$$A' = -\frac{\cos\theta}{r} + r\cos\theta + \frac{1}{R_M{}^{\frac{1}{2}}} A'_1 + \dots,$$

$$u(\varphi) = u_1(\varphi) + \frac{1}{R_M{}^{\frac{1}{2}}} u_2(\varphi) + \dots,$$

the leading term in (29) gives

$$u_1(\varphi) = -\frac{2\varphi}{\pi(1-\varphi^2)^{\frac{1}{2}}}, \tag{32}$$

and the value of A on the cylinder is

$$A = -\left(\frac{2}{\pi R_M}\right)^{\frac{1}{2}} \int_{1}^{\varphi} \frac{\xi\, \mathrm{d}\xi}{(1-\xi^2)^{\frac{1}{2}}(\varphi-\xi)^{\frac{1}{2}}}. \tag{33}$$

This integral can be expressed in terms of K and E, the first and second complete elliptic integrals, giving

$$A = -\frac{2}{(\pi R_M)^{\frac{1}{2}}}[K(\cos\tfrac{1}{2}\theta) - 2E(\cos\tfrac{1}{2}\theta)], \tag{34}$$

where $\cos\theta = \varphi$. Thus on the cylinder the potential varies from $(\pi/R_M)^{\frac{1}{2}}$ at the front stagnation point, $\theta = \pi$, to 0 at the point $\theta \simeq 49°$ and is negative for smaller values of θ. The expression (34) tends to infinity at the rear stagnation point. The correct value at this point, $\theta = 0$, is given by (30) as

$$-\frac{2}{\pi}\int_{-1}^{1} \frac{\xi}{(1-\xi^2)^{\frac{1}{2}}} \exp[R_M(1-\xi)]\, K_0[R_M(1-\xi)]\, \mathrm{d}\xi, \tag{35}$$

and the divergent integral arises when the asymptotic value of the Bessel function is used at $\xi = 1$. To evaluate (35) more accurately, the integral can be divided into two parts, in one of which the asymptotic expansion can be used. If it is supposed that the value of $K_0(x)$ is given by the first term of the asymptotic expansion to sufficient accuracy when $x > \varepsilon$:

$$A = -\left(\frac{2}{\pi R_M}\right)^{\frac{1}{2}} \int_{-1}^{1-\varepsilon/R_M} \frac{\xi \,\mathrm{d}\xi}{(1-\xi^2)^{\frac{1}{2}}\,(1-\xi)^{\frac{1}{2}}} - \frac{2}{\pi} \int_{1-\varepsilon/R_M}^{1} \frac{\xi}{(1-\xi^2)^{\frac{1}{2}}} \cdot$$
$$\cdot \exp\,[R_M(1-\xi)]\; K_0[R_M(1-\xi)]\,\mathrm{d}\xi =$$
$$= -\frac{1}{(\pi R_M)^{\frac{1}{2}}} \ln R_M + O(R_M{}^{-\frac{1}{2}}),$$

on evaluating the first integral, the second being of order $R_M{}^{-\frac{1}{2}}$. The value of the potential on the cylinder thus tends to 0 as $R_M \to \infty$ at all points, but it becomes relatively more concentrated near the rear stagnation point.

As before, A is exponentially small except within the boundary layer and the wake, defined by (22). In the boundary layer,

$$A = -\left(\frac{2}{\pi R_M}\right)^{\frac{1}{2}} \int_{-1}^{\varphi} \frac{\xi}{(1-\xi^2)^{\frac{1}{2}}(\varphi-\xi)^{\frac{1}{2}}} \exp[-R_M\psi^2/2(\varphi-\xi)]\,\mathrm{d}\xi, \tag{36}$$

and the value in the wake is given by the same expression with the upper limit of integration 1. The forms obtained for these integrals by making the transformations (23) are not particularly simple and so are omitted. The value of the potential in the wake at a large distance downstream is found to be

$$A = -\left(\frac{\pi}{R_M}\right)^{\frac{1}{2}} x^{-\frac{3}{2}} \exp(-\,R_M y^2/4x) \tag{37}$$

in the same way as (28) was found.

In the limiting case, as R_M tends to infinity, there is a tangential component of magnetic field, $H_\theta = -2\cos\theta$, on the cylinder. In the wake, the y-component of the magnetic field tends to 0, but the x-component

$$H_x = \frac{\partial A}{\partial y} = \left(\frac{\pi R_M}{4}\right)^{\frac{1}{2}} y x^{-\frac{5}{2}} \exp(-\,R_M y^2/4x)$$

has a maximum value $(\pi/2e)^{\frac{1}{2}}\, x^{-2}$ at $y = (2x/R_M)^{\frac{1}{2}}$ and a corresponding minimum at $y = -\,(2x/R_M)^{\frac{1}{2}}$. In the limit, the magnetic field in the wake lies along the axis and is directed away from and towards the cylinder on opposite sides of the axis. A sketch of the magnetic lines for large R_M is given in fig. 2.

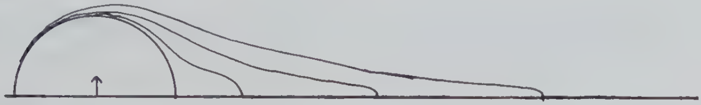

Fig. 2. The magnetic lines when the dipole is perpendicular to the stream. (N.B. This is a rough sketch intended to give qualitative information only).

§ 4. *The modified velocity field and the drag.* The magnetic field in the fluid produces a non-conservative body force which generates vorticity and so modifies the velocity field. The equation determining this modification is (3), which leads to

$$\omega = -\frac{1}{2}\frac{\partial P_1}{\partial \psi} + R_M H_\phi H_\psi, \tag{38}$$

$$0 = -\frac{1}{2}\frac{\partial P_1}{\partial \varphi} - R_M H_\psi{}^2, \tag{39}$$

where ω is the vorticity, perpendicular to the plane of motion, p_1 and $\boldsymbol{q}_1$ are the additional pressure and velocity terms, $P_1 = p_1 + \boldsymbol{q}_0 \cdot \boldsymbol{q}_1$, and H_ϕ and H_ψ are the φ- and ψ-components of the magnetic field. Since ω must vanish at a large distance upstream, *i.e.* at $\varphi = -\infty$, the terms in P_1 can be eliminated giving

$$\omega - R_M H_\phi H_\psi = R_M \int_{-\infty}^{\varphi} \frac{\partial}{\partial \psi}\,(H_\psi{}^2)\,\mathrm{d}\varphi =$$

$$= R_M \frac{\partial}{\partial \psi} \int_{-1}^{\varphi} H_\psi{}^2\,\mathrm{d}\varphi, \tag{40}$$

since $H_\psi = 0$ when $\varphi < -1$.

The vorticity is negligible except in the boundary layer and the wake, a narrow region on either side of the line $\psi = 0$. This surface distribution of vorticity can be replaced by a line distribution on $\psi = 0$, the strength at any point being determined by integrating

ω across the region, *i.e.* from $\psi = 0$ to $\psi = \infty$ on the upper surface of the cylinder, from $\psi = 0$ to $\psi = -\infty$ on the lower surface, and from $\psi = -\infty$ to $\psi = \infty$ in the wake. From this distribution of vortex filaments, the velocity can be found and an irrotational velocity field can then be added to satisfy the boundary conditions on the cylinder and at infinity.

For the dipole pointing upstream, the magnetic field is determined by (24). The vorticity density on the upper surface is given by

$$\tilde{\omega} = \int_0^\infty \omega \,\mathrm{d}\psi = R_M \int_0^\infty H_\psi H_\phi \,\mathrm{d}\psi + \left[R_M \int_{-1}^{\varphi} H_\psi{}^2 \,\mathrm{d}\varphi\right]_{\psi=0}^{\psi=\infty}$$

using (40), and substituting the values found from (24),

$$\tilde{\omega}(\varphi) = 1 - \varphi^2 - \frac{1}{\pi}(3 + 2\varphi - \varphi^2). \tag{41}$$

On the lower surface, the sign is reversed, and since the vorticity has opposite signs on either side of the downstream axis, the vorticity density along the axis is zero. The velocity field produced by this vorticity distribution can be found in the usual way by summing the velocities produced at any point by each vortex filament. On the cylinder, the velocity produced at the point θ by the filaments at $\theta = \pm\,\theta_1$ is directed radially outwards and is of magnitude

$$\frac{\tilde{\omega}(\cos\theta_1)}{2\pi}\,[\cot\tfrac{1}{2}(\theta_1 - \theta) + \cot\tfrac{1}{2}(\theta_1 + \theta)],$$

so that the velocity field produced by the vorticity has only a radial component on the cylinder,

$$\tilde{q}_r = \frac{1}{2\pi}\int_0^\pi \frac{\tilde{\omega}(\cos\theta_1)\sin\theta_1}{\cos\theta_1 - \cos\theta}\,\mathrm{d}\theta_1. \tag{42}$$

Since the total strength of the vorticity is zero, the velocity is $O(1/r^2)$ at large distances from the cylinder. The irrotational field to be added to this must vanish at infinity and make the total radial component zero on the cylinder. It can be derived from a potential of the form

$$\chi = \sum_{n=1}^{\infty} \frac{a_n \cos n\theta}{r^n},$$

and the boundary condition $\partial\chi/\partial r = -\tilde{q}_r$ on $r = 1$ gives

$$\sum_{n=1}^{\infty} n a_n \cos n\theta = \frac{1}{2\pi}\int_0^{\pi} \frac{\tilde{\omega}(\cos\theta_1)\sin\theta_1}{\cos\theta_1 - \cos\theta}\,\mathrm{d}\theta_1, \tag{43}$$

which determines the coefficients a_n.

The pressure on the cylinder is found by integrating (39), which gives

$$p_1 + 2\sin\theta \sum n a_n \sin n\theta = -2R_M \int_{-1}^{\varphi} H_\psi{}^2\,\mathrm{d}\varphi = -\frac{1}{\pi}(3 + 2\varphi - \varphi^2).$$

The drag on the cylinder is produced by the pressure and the Maxwell stress. The pressure drag can be written $\rho U^2 L D_P$, where D_P is a non-dimensional drag coefficient

$$D_P = -\beta \int_0^{2\pi} p_1 \cos\theta\,\mathrm{d}\theta = \beta(2 + 2\pi a_2). \tag{44}$$

The coefficient a_2 is found from (43) to be

$$a_2 = \frac{1}{2\pi^2}\int_0^{\pi}\int_0^{\pi} \frac{\tilde{\omega}(\cos\theta_1)\sin\theta_1\cos 2\theta}{\cos\theta_1 - \cos\theta}\,\mathrm{d}\theta\,\mathrm{d}\theta_1 = \frac{4}{3\pi^2},$$

so that

$$D_P = \beta\left(2 + \frac{8}{3\pi}\right). \tag{45}$$

The Maxwell stress produces a drag with coefficient

$$D_M = \beta \int_0^{2\pi} [\tfrac{1}{2}(H_r{}^2 - H_\theta{}^2)\cos\theta - H_r H_\theta \sin\theta]\,\mathrm{d}\theta,$$

and substituting the value of the magnetic field on the cylinder,

$$D_M = \frac{128\beta}{15}\left(\frac{\mu' + \mu}{\mu'}\right)\left(\frac{\pi}{R_M}\right)^{\frac{1}{2}}. \tag{46}$$

The pressure drag is of larger order than the Maxwell drag and is independent of R_M, so that (45) is the value of the drag when R_M is infinite. This drag is produced by the magnetic forces, not directly by means of the Maxwell stress, but through the production of vorticity and the consequent modification of the pressure. It is interesting to note that the drag on the cylinder for infinite R_M is proportional to $\beta\rho U^2 L = \mu h^2 L$ and so is independent of the stream velocity. This does not mean that the force is non-zero when the fluid is at rest, since the analysis is based on the supposition that $\mu h^2/\rho U^2$ is small.

When the dipole is perpendicular to the free stream, the more complicated form for the magnetic field and the difficulty of removing the infinity at the rear stagnation point make the determination of the velocity field and the pressure too difficult to be accomplished by analytic methods. The Maxwell drag can be found using (29) and (34), giving a drag coefficient

$$D_M = 4.15\beta\left(\frac{\mu + \mu'}{\mu'}\right) R_M{}^{-\frac{1}{2}},$$

but the pressure drag may be expected to be of higher order than this, as in the previous case.

I would like to express my indebtedness to Dr. J. D. Murray for his help and encouragement during the preparation of this paper.

Received 26th January, 1961.

REFERENCES

1) Ludford, G. S. S. and J. D. Murray, J. Fluid Mech **7** (1960) 516.
2) Murray, J. D. and L. K. Chi, Mathematika **7** (1960) 64.
3) Michael, D. H., Mathematika **1** (1954) 131.
4) Piercy, N. A. V. and H. F. Winny, Phil. Mag. (7) **16** (1933) 390.

FILED IN STACKS

MARTINUS NIJHOFF — PUBLISHER — THE HAGUE

MICROPROJECTION WITH X-RAYS

by

ONG SING POEN

TECHNOLOGICAL UNIVERSITY, DELFT

One of the 5 types of X-ray microscopes is the projection microscope, originally proposed by Von Ardenne in 1939 and realized by Cosslett and Nixon in 1951.

With the aid of an ultra-fine-focus X-ray tube with a spot diameter of 1–0.1 micron, an enlarged X-ray shadow image is projected on a screen or film. Due to negligible scattering and refraction clear absorption images can be obtained. A special feature is the great depth of focus. Thus ideal stereo images can be made, showing the three dimensional mass absorption distribution of the specimen. This will be of great importance for both research (medical, biological, metallurgical, criminological, etc.) and technology (rubber-, textile-, paper-industry etc.).

In "Microprojecton with X-rays" the author describes his experiences in constructing and applying the projection microscope in practice, covering five years of research in this field. His book will serve as a guide to those who are intending to explore the possibilities of this type of microscope.

1959. 132 pages on art paper. With 42 figures and 38 illustrations.
Guilders 12.50

Obtainable through any bookseller or from the publisher